International Journal of Nanomedicine

Dovepress
open access to scientific and medical research

Open Access Full Text Article

ORIGINAL RESEARCH

Pulmonary delivery of transferrin receptors targeting peptide surface-functionalized liposomes augments the chemotherapeutic effect of quercetin in lung cancer therapy

This article was published in the following Dove Press journal:
International Journal of Nanomedicine

Muhammad Kashif Riaz[1]
Xue Zhang[1]
Ka Hong Wong[1]
Huoji Chen[2]
Qiang Liu[2]
Xiaoyu Chen[1]
Ge Zhang[1]
Aiping Lu[1,3]
Zhijun Yang[1,3]

[1]School of Chinese Medicine, Hong Kong Baptist University, Hong Kong, People's Republic of China; [2]School of Traditional Chinese Medicine, Southern Medical University, Guangzhou, People's Republic of China; [3]Changshu Research Institute, Hong Kong Baptist University, Changshu Economic and Technological Development (CETD) Zone, Changshu, Jiangsu Province, People's Republic of China

Purpose: Lung cancer has a high incidence rate worldwide with a 5-year survival rate of 18%, and is the leading cause of cancer-related deaths. The aim of this study is to augment therapeutic efficacy of quercetin (QR) for lung cancer therapy by targeting transferrin receptors, which are overexpressed and confined to tumor cells.

Methods: In this study, T7 surface-functionalized liposomes loaded with QR (T7-QR-lip) having different T7 peptide densities (0.5%, 1% and 2%) were prepared by the film hydration method. T7 surface-functionalized liposomes were characterized and evaluated in terms of in vitro cytotoxicity and cellular uptake, 3D tumor spheroid penetration and inhibition capabilities, in vivo biodistribution and therapeutic efficacy in mice with orthotopic lung-tumor implantation by fluorescent and bioluminescent imaging via pulmonary administration.

Results: In vitro, 2% T7-QR-lip exhibited significantly augmented cytotoxicity (~3-fold), higher apoptosis induction and S-phase cell-cycle arrest. A prominent peak right-shift and enhanced mean fluorescence intensity was observed in A549 cells treated with T7 Coumarin-6 liposomes (T7-Cou6-lip), confirming the target specificity of T7 targeted liposomes; while, after treatment with T7-QR-lip and non-targeted QR-lip, no significant difference was observed in cellular uptake and in vitro cytotoxicity studies in MRC-5 (normal lung fibroblast) cells. T7-Cou 6-lip showed higher fluorescence intensity in A549 cells and a significantly deeper penetration depth of 120 μm in the core of the tumor spheroids and T7-QR-lip produced significantly higher tumor-spheroid growth inhibition. The in vivo biodistribution study via pulmonary delivery of T7 1,1'-dioctadecyltetramethyl-indotricarbocyanine iodide liposomes demonstrated liposome accumulation in the lungs and sustained-release behavior up to 96 h. Further, T7-QR-lip significantly enhanced the anticancer activity of QR and lifespan of mice ($p<0.01$, compared with saline) in orthotopic lung tumor-bearing mice via pulmonary administration.

Conclusion: T7 surface-functionalized liposomes provide a potential drug delivery system for a range of anticancer drugs to enhance their therapeutic efficacy by localized (pulmonary) administration and targeted delivery.

Keywords: Quercetin, lung cancer, surface-functionalized liposomes, T7 peptide, orthotopic lung cancer model, pulmonary delivery

Correspondence: Zhijun Yang
School of Chinese Medicine, Hong Kong Baptist University, 7 Baptist University Road, Kowloon Tong, Kowloon, Hong Kong, People's Republic of China
Email yzhijun@hkbu.edu.hk

Introduction

Lung cancer has a high global incidence rate and is the leading cause of cancer-related mortalities. In 2018, lung cancer was estimated to be responsible for

1.76 million deaths worldwide out of all (9.6 million) cancer-related deaths.[1] It has been estimated that in 2018 lung cancer caused ~84,000 (26% of the cancer cases) deaths in the USA. The 5-year survival rate for lung cancer has been estimated to be 18%.[2] Lung cancer was among four major cancers (lung cancer, breast cancer, colon cancer and prostate cancer) causing cancer-related deaths.[3] The two main types of lung cancer are non-small-cell lung cancer (NSCLC) and small-cell lung cancer, contributing to ~85% and ~15% of lung cancer cases, respectively.[4] Lung computed tomography scans are helpful in the detection of early stage cancers,[5] and the cessation of smoking is recommended to decrease the lung cancer mortality rate.[6] Therefore, efficient treatment for lung cancer with less adverse effects is the need of the hour. In this connection, pulmonary delivery could provide a localized response of antitumor drugs to the lungs as compared to the enhanced-permeability and retention effect, minimizing the adverse effects on other organs by retention of the drug in the lungs.[7–13]

In order, to enhance tumor-specific drug delivery and avoid off-target effects, active targeting is the current approach and has proven to be an efficient strategy.[14] The active targeting approach involves preparation of targeted liposomes, by surface functionalization of liposomes with a suitable targeting ligand (monoclonal antibody, peptide, etc).[15–23] Various receptors are overexpressed in cancer cells.[24,25] Although expression of transferrin receptor (TFR) is low in most normal cells, it is overexpressed (~100-fold) in many cancers such as ovarian, brain, breast, lung adenocarcinoma, prostate, etc due to increased iron demand.[26,27] TFRs are transmembrane proteins,[28] and transferrin (TF) (iron binding protein of ~80 kDa) specifically binds to TFRs overexpressed on the surface of cancer cells, resulting in receptor-mediated endocytosis and uptake of iron to fulfill the metabolic needs of cancer cells.[15,29] TFRs have high expression in the A549 cell line. This fact has been supported by a study on TF-conjugated liposomes loaded with doxorubicin for treatment of lung cancer (A549 cells). TF-conjugated liposomes showed higher uptake in A549 cells.[30] In a study, increased cytotoxicity of TFR-targeted docetaxel liposomes was observed as compared to non-targeted docetaxel liposomes.[31] In another study, it was suggested that targeting of TFR to cancer cells can be done using TF antibodies (and their fragments) and specific peptides, resulting in cancer growth inhibition or apoptosis induction in a variety of cancers.[28]

T7 (HAIYPRH) peptide, identified by phage display and enriched with a biopanning process, is a cell-targeting peptide having specific binding affinity for TFR.[32] T7 peptide targets a small cavity on the TFR surface and then is transported inside the cell through endocytosis with the help of TF.[26] T7 peptide has an advantage in targeting the TFR, ie, it does not compete with TF (serum iron-carrier protein) for binding to TFR.[32,33] In a study, artemisinin and T7 conjugate showed potent anticancer activity against molt-4 leukemia cells by targeting overexpressed TFRs, and co-internalization of artemisinin and TF.[34] Wu et al[35] have reported the preparation of T7-functionalized liposomes containing paclitaxel, which showed cytotoxicity against ovarian cancer (A2780 cells). Doxorubicin-loaded liposomes functionalized by TAT (a cell-penetrating peptide) and T7 peptide have been reported for brain tumor ie, treatment of glioma, which is difficult to treat due to the low permeability of drug delivery systems across the blood–brain barrier.[3636] Dual peptide-modified (T7 peptide and DA7R peptide) liposomes were prepared for the co-delivery of anticancer drugs (doxorubicin and vincristine) and these liposomes in vivo showed an antiglioma effect.[37] In another study, it was reported that T7-directed liposomes containing ZL006 (neuroprotectant) could be used as a potential targeted drug delivery system for (ischemic) stroke treatment.[33] Therefore, T7 peptide appears to be a promising targeting ligand for overexpressed TFRs in cancer cells.

Quercetin (QR), 3,5,7,3′,4′-pentahydroxylflavone, is a natural flavonoid widely distributed in nature and is known to possess anticancer activity,[38] ie, it inhibits the growth of lung cancer (A549 cells),[39] colon cancer,[40] breast cancer,[38] etc. QR is present in edible fruits and vegetables (eg, apples, grapes, onions, etc).[38,41] QR exhibits anticancer activity in lung cancer (A549 cells) by activation of the MEK–ERK pathway along with inactivation of Akt-1 and variation in expression of Bcl-2 family (proteins).[42] QR suppresses the growth of a variety of NSCLC cell lines by inhibiting overexpressed Aurora-B kinase and can be used for lung cancer therapy.[43] However, the application of QR in lung cancer therapy has been restricted by a number of factors, ie, low water solubility (2.15 μg/mL), low bioavailability and rapid clearance from plasma.[44,45] QR utilization as a chemoprevention drug has been suggested because it is involved in cell-cycle arrest, apoptosis, replication and angiogenesis.[46] QR-mediated cell-cycle arrest and apoptosis in human breast cancer MCF-7 cells have been reported.[47] QR liposomes made from DSPE-PEG(2000) have been shown to be effective in inhibiting the growth

of glioma cells as compared to free QR.[48] Therefore, we have explored the utility of peptide-functionalized liposomes as a nanocarrier to overcome the limitations of QR in lung cancer therapy.

In this work, various types of QR-loaded liposomes (T7 targeted liposomes) with different peptide densities ie, 0.5%, 1% and 2% and non-targeted liposomes were successfully formulated with an aim to actively and passively target the QR-loaded liposomes to lung cancer sites. Further, we are reporting for the first time the application of T7 targeted liposomes containing QR for lung cancer treatment using pulmonary delivery and bioluminescent imaging in BALB/c nude mice bearing orthotopic lung-tumor implantation. A hydrophobic drug ie, QR was encapsulated in the lipid bilayer of the liposomes. To confer the targeting ability to liposomes, DSPE-PEG(2000)-MAL was first conjugated to the distal end of T7 peptide. T7 targeted liposomes loaded with QR were then formulated using the conjugate and were characterized, ie, particle size, polydispersity, encapsulation efficiency (%) and stability study. In vitro cytotoxicity and target specificity evaluation of T7 targeted liposomes by cellular uptake studies were performed in lung cancer (A549 cells) and normal lung (MRC-5 cells) using a confocal microscope and flow cytometer. The cytotoxic effects of T7 surface-functionalized liposomes loaded with QR (T7-QR-lip) were further confirmed in A549 cells by cell-cycle analysis and apoptosis study. The penetration and inhibition ability of T7 targeted liposomes were evaluated after treatment of 3D lung tumor spheroids with T7 Coumarin-6 liposomes (T7-Cou6-lip) and T7-QR-lip, respectively. An in vivo biodistribution study was performed by fluorescent imaging at different time points after pulmonary delivery of T7 1,1'-dioctadecyltetramethyl-indotricarbocyanine iodide liposomes (T7-DiR-lip) in orthotopic lung tumor-bearing BALB/c nude mice using an IVIS Lumina XR system. Furthermore, the in vivo therapeutic efficacy of T7-QR-lip via pulmonary administration was examined in BALB/c nude mice with orthotopic lung-tumor implantation by bioluminescent imaging and bioluminescence-signal monitoring using the IVIS Lumina XR system. This study provides an insight into the biodistribution behavior and therapeutic potential of T7 peptide surface-functionalized liposomes for targeted and sustained delivery of a drug ie, QR through pulmonary administration in lung cancer therapy.

Materials and methods

Materials

T7 peptide with a terminal cysteine (Cys-HAIYPRH) was synthesized by Genscript USA Inc. (Piscataway, NJ, USA). Soybean lecithin (SPC) was purchased from Shanghai Tai-Wei Chemical Company (Shanghai, China). QR was purchased from Tocris Bioscience (Bristol, UK). DSPE-PEG (2000) (ammonium salt) was purchased from Avanti-Polar Lipids Inc. (Alabaster, AL, USA). DSPE-PEG-MAL (SUNBRIGHT® DSPE-020MA) was purchased from NOF America (White Plains, NY, USA). 3-(4,5-Dimethylthiazol-2-yl)-2,5-diphenyltetrazolium bromide (MTT) was supplied by Invitrogen (Thermo Fisher Scientific, Waltham, MA, USA). Coumarin-6 (Cou6) and dimethyl-sulfoxide (DMSO) were purchased from Sigma-Aldrich Co. (St Louis, MO, USA). Hoechst-33,342 and LysoTracker Red DND-99 (fluorescent dyes) were supplied by Molecular Probes Inc. (Eugene, OR, USA). 1,10-Dioctadecyltetramethyl-indotricarbocyanine iodide (XenoLight DiR), a near-infrared lipophilic carbocyanine dye, was purchased from Caliper Life Sciences (Hopkinton, MA, USA). D-Luciferin (potassium salt) was purchased from Cayman Chemicals (Ann Arbor, MI, USA). Ultrapure water was obtained by a Milli-Q® water purification system (Merck Millipore, Billerica, MA, USA). All other chemicals were of analytical grade.

Cells and animals

A549-luciferase (A549-Luc) cells were purchased from PerkinElmer, Inc. (Waltham, MA, USA). The NSCLC cell line (A549 cells) was kindly provided by the Department of Anatomical and Cellular Pathology, The Chinese University of Hong Kong and use of the cell line was permitted by the Laboratory Safety Committee, School of Chinese Medicine, Hong Kong Baptist University and Department of Health, Hong Kong. Male BALB/c nude mice (7–8 weeks old) were purchased from the Laboratory Animal Services Centre, The Chinese University of Hong Kong. All animal experiments were approved by the Health Department of Hong Kong (Special Administrative Region) and the experiments were carried according to the Guidelines of the Committee on the use of Human and Animal Subjects in Teaching and Research of Hong Kong Baptist University. Anesthesia was performed (before experiment) with an intraperitoneal injection of chloral hydrate at a dose of 150 mg/kg.

Synthesis of DSPE-PEG(2000)-MAL-T7

T7 peptide (HAIYPRH) with terminal cysteine was conjugated with DSPE-PEG-MAL micelles by incubation of T7 peptide dissolved in PBS (pH 7.4) with DSPE-PEG-MAL micelles (1:1 molar ratio) in a glass vial at room temperature with 48 h gentle agitation. Purification of the resultant DSPE-PEG-MAL-T7 was done by dialysis (molecular weight cut-off 3.5 kDa) with purified water for 48 h. DSPE-PEG-MAL -T7 purified by dialysis was then freeze dried for 72 h. Lyophilized DSPE-PEG-MAL-T7 was stored at −20 °C for use in the preparation of T7 surface-functionalized liposomes.

In order to perform matrix-assisted laser desorption/ionization–time of flight mass spectrometry (MALDI-TOF-MS), 0.5 µL of sinapinic acid solution in ethanol was deposited on the MALDI target plate and allowed to dry. Further, the analyte was mixed with sinapinic acid solution in 30% (v/v) acetonitrile solution in water (1:1 ratio). Finally, 0.5 µL of analyte/matrix mixture was deposited on the matrix spot and allowed to dry. The formation of DSPE-PEG(2000)-MAL-T7 was confirmed using a MALDI-TOF mass spectrometer (Autoflex III; Bruker-Daltonics Inc., MA, USA). The successful synthesis of DSPE-PEG(2000)-MAL-T7 was confirmed with right-shift of the DSPE-PEG(2000)-MAL peak and the corresponding mass–charge ratios.

Formulation of T7 targeted liposomes

Liposomes were prepared by the film hydration method. Non-targeted (PEGylated) liposomes (QR-lip) contained soy-phosphatidylcholine (SPC), DSPE-PEG(2000), cholesterol and anticancer drug ie, QR (molar ratio 25:1.31:3.0:2.5, respectively). In addition to the above constituents, T7 targeted liposomes (T7-QR-lip) contained DSPE-PEG(2000)-MAL-T7 conjugate at 0.5%, 1.0% and 2.0% molar ratios to the total lipid concentration to formulate 0.5%, 1.0% and 2.0% T7 targeted liposomes. Briefly, 2% T7 targeted liposomes (T7-QR-lip) contained SPC, DSPE-PEG(2000), DSPE-PEG(2000)-MAL-T7, cholesterol and QR (molar ratio 25:1.05:0.26:3.0:2.5, respectively).

The constituents were dissolved in a 5 mL mixture of chloroform and methanol (2:1 v/v) to formulate the liposomes. A dry lipid film was formed on the walls of a round-bottom flask by evaporation of the mixture of organic solvents using a rotary evaporator. The dry lipid film was hydrated with 10 mL of PBS buffer at 65 °C for 30 min. The resulting liposomal suspension (multilamellar vesicles) was extruded five times through 0.2 µm, 0.1 µm and 0.08 µm pore-size filters under nitrogen gas using LIPEX Extruder (NorthernLipids, Vancouver, Canada). Cou6 liposomes and 1,1'-dioctadecyltetramethyl-indotricarbocyanine iodide (DiR) liposomes contained the dye instead of the anticancer drug (QR). Cou6 dye and DiR (lipophilic near IR) dye have been used to study the in vitro cellular uptake and in vivo biodistribution of T7 targeted liposomes. The abbreviations for T7 QR liposomes, T7 Coumarin-6 liposomes and T7 DiR liposomes have been described as T7-QR-lip, T7-Cou6-lip and T7-DiR-lip, respectively. Non-targeted liposomes were formulated using the same procedure, but without T7 peptide.

Characterization of liposomes: particle size, polydispersity index, encapsulation efficiency and stability study

Particle size distribution and the polydispersity index (PDI) of the liposomes were assessed using the Delsa Nano-HC Particle Analyzer (Beckman Coulter, CA, USA). QR-loaded liposomes (20 µL) were diluted with methanol (980 µL) to induce drug release and the QR concentration in liposomes was determined by ultra-performance liquid chromatography (UPLC; Waters, MA, USA) using an ACQUITY-UPLC BEH C18 column (1.7 µm, 2.1 mm×50 mm). The mobile phase was composed of methanol and water (45:55% v/v) containing 0.1% formic acid.

The ultrafiltration technique was used to determine the encapsulation efficiency of QR liposomes, as previously reported.[16] QR liposomal formulations (250 µL) were placed in the upper chamber of an Amicon Ultra (0.5) centrifugal filter (10K cut-off) (EMD Millipore, Billerica, MA, USA) and centrifugation was done at 10,000 rpm for 15 min. Quantification of unencapsulated QR in the ultra-filtrate was done using UPLC with UV detection at 256 nm. The following equation was used to calculate the encapsulation efficiency (%):

$$EE(\%) = \frac{\text{Weight of total Quercetin} - \text{Weight of unencapsulated Quercetin}}{\text{Weight of total Quercetin}} \times 100\%$$

Stability study of QR liposomes was done at 4 °C by measuring the particle size and PDI, at the predetermined time points.

In vitro drug release study

The in vitro drug release study was performed by the dialysis method. One milliliter of free QR solution, QR-

lip and 2% T7-QR-lip at a uniform QR concentration was placed in a dialysis bag (molecular weight cut-off 12–14 kDa) and sealed. Dialysis bags were immersed in 10 mL of 10% ethanol solution, as previously reported with little modification.[67] Various QR liposomal formulations were incubated at 37 °C with mild oscillations at 100 rpm for 96 h. Then, 100 µL of release medium was sampled and refilled with 100 µL of fresh medium at specific time intervals ie, 1, 2, 4, 8, 24, 48, 72 and 96 h. The QR concentration in the release medium was determined by UPLC.

In vitro cytotoxicity study of T7 targeted liposomes by MTT assay

MTT assay was done to evaluate the in vitro cytotoxicity of various QR formulations, ie, T7 targeted liposomes (T7-QR -lip), non-targeted (PEGylated) liposomes (QR-lip) and free QR solution, on A549 (lung cancer) cells and MRC-5 (normal lung fibroblast) cells. QR stock solution was prepared by dissolving QR in DMSO for use in the experiment. The cells (A549 and MRC-5) were seeded in a 96-well plate at a density of 6×10^3 cells per well and allowed to grow overnight in an incubator at 37 °C. After 24 h of incubation, the medium was removed and the wells were washed twice with PBS. After washing the wells with PBS, various formulations of T7-QR-lip, QR-lip and free QR solution with QR concentrations of 3.25–100 µM were added to each well after diluting the original formulations in fresh medium. The incubation with various QR formulations was done at 37 °C for 48 h.

After 48 h of incubation with different QR formulations, 20 µL of MTT solution (5 mg/mL in PBS) was added to each well and incubation was done for 4 h in an incubator at 37 °C. MTT in the medium was removed and DMSO (100 µL/well) was added to dissolve the formazan crystals. The MTT plate was covered with aluminum foil and shaking was done for 15 min by placing on a shaker. Absorbance was measured at 570 nm using a Benchmark Plus Microplate-Reader (Bio-Rad Laboratories Inc., Hercules, CA, USA) and the cell viability was calculated.

In vitro cytotoxicity investigation of T7 targeted liposomes by apoptosis study

The method has been described previously,[16] which was used with some alteration. In this study, A549 cells were seeded in a six-well plate at a density of 5×10^5 cells per well with incubation at 37 °C for 24 h. Then, the medium was removed and the wells were washed twice with PBS. After washing the wells with PBS, T7-QR-lip, QR-lip and free QR solution at a concentration of 50 µM were added to each well after diluting the original formulations in fresh medium. After 24 h of incubation, the medium was removed and 0.5 mL trypsin was added to each well, followed by incubation for a few minutes to detach the cells. Addition of fresh medium was done into each well and then the contents of each well transferred into test tubes. The cells were centrifuged in each test tube at 1000 rpm for 5 min. The supernatant was removed and the cells were washed with PBS twice, followed by centrifugation at 1000 rpm for 5 min. Cells were resuspended in binding buffer. Then, 100 µL ($2x10^5$ cells) of the cells suspended in binding buffer were transferred to the flow cytometry tubes. Addition of 5 µL FITC Annexin-V and 5 µL propidium iodide (PI) to the flow cytometry tubes followed. The cells were slightly vortexed and incubated for 15 min in the dark. Addition of 400 µL binding buffer was done to the flow cytometry tubes. The cells stained with two dyes were analyzed with the flow cytometer for the acquisition of 10,000 events per histogram.

In vitro cytotoxicity study of T7 targeted liposomes by cell-cycle analysis study

Briefly, A549 cells were seeded at a density of 5×10^5 cells on six-well culture plates, and allowed to grow for 24 h in an incubator at 37 °C. After 24 h of incubation, cells were treated with PBS, T7-QR-lip, QR-lip and free QR solution at a concentration of 50 µM for 24 h. Then, the cells were trypsinized and washed twice with cold PBS. Cells were resuspended in 70% ethanol and fixed by overnight incubation at 4 °C. The fixed cells were pelleted and resuspended in 1 mL of staining solution containing PI, RNase and 1× PBS. Twenty-thousand fixed cells were analyzed on a FACSCalibur system (BD Biosciences, San Jose, CA, USA). The cell-cycle profiles were analyzed using ModFit program version 3.1 (Verity Software House, ME, USA).

Cellular uptake study (in vitro target specificity) of T7 targeted liposomes

The cellular uptake of liposomes by A549 cancer cells was studied by confocal-laser scanning microscope (CLSM) and flow cytometry.

Cellular uptake of liposomes (qualitative study) by CLSM

A549 cells were seeded on a glass-bottomed dish at a density of 1×10^5 cells/mL and grown overnight by incubation at 37 °C for 24 h. After 24 h the medium was replaced with full medium containing liposomal formulations, ie, T7 targeted Coumarin-6 liposomes (T7-Cou6-lip), Coumarin-6 liposomes (Cou-6 lip) and free Coumarin-6 (Cou-6) dye (green fluorescence) at a concentration of 0.1 μg/mL, followed by incubation at 37 °C for 3 h. LysoTracker Red (red fluorescence) was added to the cells at a concentration of 50 nM and incubation was done for half an hour at 37 °C to stain the lysosmes. Cells were washed three times with PBS followed by fixation of the cells by treatment with 4% paraformaldehyde for 20 min. The cells were again washed three times with PBS and treatment was done with 2.5 μg/mL of Hoechst-33,342 (blue fluorescence) at 37 °C for 15 min to counterstain the cell nuclei. The cells were again washed with PBS and visualized by CLSM. Higher green fluorescence intensity of Cou6 dye in the images taken from CLSM indicates higher cellular uptake of T7-Cou6-lip as compared to Cou6-lip and free-Cou6 dye.

Cellular uptake of liposomes (quantitative study) by flow cytometry

A549 cells were seeded on six-well assay plates at 5×10^5 cells per well and grown overnight by incubation at 37 °C for 24 h. After 24 h the medium was replaced with medium containing liposomal formulations, ie, T7-Cou6-lip, Cou-6 lip and free Cou6-dye at a concentration of 0.1 μg/mL, followed by incubation at 37 °C for 3 h. The cells were washed with PBS three times, followed by trypsinization. The trypsinized cells were centrifuged at 1000 rpm for 5 min. Finally, cells were resuspended in 0.5 mL PBS. The fluorescent intensity of the treated cells was determined using a FACSCanto flow cytometer (Becton-Dickinson, NJ, USA), by the acquisition of 10,000 events per histogram.

Tumor-spheroid penetration and inhibition study

In vitro development of 3D lung tumor spheroids

A549 cell 3D spheroids were formed by the hanging drop method with little modification.[49] The 96-well culture plates were precoated with 80 μL of 2% (w/v) agarose in FBS-free medium with subsequent incubation in an incubator at 37 °C with 5% CO_2. A549 cells at a concentration of 1×10^3 cells in 200 μL of DMEM with FBS medium were seeded in each well of a 96-well plate. The 3D tumor spheroids were daily monitored and photographed using an inverted phase-contrast microscope. Compact and uniform tumor spheroids were selected for further use in 3D tumor-spheroid penetration and growth inhibition experiments.

3D lung tumor-spheroid penetration capability study of T7 targeted liposomes

The technique has been previously described,[16,21] and was used with some modifications. Uniform and compact tumor spheroids with a diameter of >300 μm were selected and transferred to a confocal dish for use in the experiment. Tumor spheroids were incubated at 37 °C for 24 h with 2% T7-Cou6-lip, Cou-6 lip and Cou6-dye at a coumarin concentration of 0.5 μg/ml. Tumor spheroids were washed with cold PBS followed by fixation with 4% paraformaldehyde solution. The spheroids were scanned from the top to the equatorial plane at 24-μm intervals to obtain Z-stack images and study the fluorescence intensity and penetration depth of the formulations using a CLSM (Leica TCS SP8; Leica Microsystems, Wetzlar, Germany).

In vitro tumor growth inhibition study in 3D lung tumor spheroids

In this study, uniform and compact tumor spheroids with a diameter of >300 μm were incubated with free QR, QR-Lip and 2% T7-QR-Lip at a QR concentration of 50 μM. The tumor spheroids were cultured for an additional 5 days. The tumor spheroids were daily imaged (at 5x magnification) using an inverted-phase microscope. The growth inhibition of tumor spheroids was then investigated by relative spheroid volume changes. Minor (d_{min}) and major (d_{max}) diameters of the tumor spheroids were recorded, and the tumor-spheroid volume was calculated using the formula: $V=0.5\times d_{max}\times d_{min}^{2.5050}$

The tumor-spheroid volume change ratio was calculated using the formula: $R = V_1/V_0\times100\%$, where V_0 and V_1 is the tumor-spheroid volume before and after treatment, respectively.

In vivo therapeutic efficacy study of T7 targeted liposomes in orthotopic lung cancer mouse models

This study involves the establishment of an A549-Luc orthotopic lung cancer mice model, biodistribution study

and therapeutic efficacy study in mice bearing orthotopic lung-tumor implantation.

Establishment of an A549-Luc orthotopic lung cancer mice model

BALB/c nude mice were implanted with A549-Luc cells using the technique as previously reported.[16,20,51] A549-luc cell suspensions (2×10^7 cells/mL) were prepared in Matrigel Matrix (BD Biosciences). The mice were anesthetized and then placed in the right-lateral decubitus position. A 1-mL syringe (with a 29-gauge needle) was used to inject 2×10^6 cells percutaneously into the right lateral thorax at the lateral dorsal axillary line.

Biodistribution of T7 targeted liposomes in vivo through pulmonary delivery

The biodistribution and tumor-targeting potential of 2% T7 targeted DiR liposomes (T7-DiR-lip) in A549-Luc orthotopic lung tumor-bearing BALB/c nude mice have been investigated with an IVIS® Lumina-XR system (Caliper Life-Sciences, MA, USA) using the technique as previously reported.[20]

Briefly, the mice were anesthetized with an intraperitoneal injection of 5% chloral hydrate at a dose of 100 µL/20 g. T7-DiR-lip at a single dose of 1 mg DiR/kg body weight was administered directly via pulmonary delivery using the Microsprayer® Aerosolizer Pulmonary Aerosol-Kit for Mouse (Penn-Century Inc., PA, USA) and the distribution behavior in the mice was monitored at different time points using the IVIS® Lumina-XR system.

Therapeutic efficacy of T7 targeted liposomes through pulmonary delivery in mice bearing A549-Luc orthotropic implantation

Orthotropic implantation of A549-Luc cells was done as described above. Seven days after A549-Luc cell implantation, mice were randomized into treatment and control groups. The nude mice were administered T7-QR-lip, QR-lip and free QR solution at a dose of 10 mg/kg, twice a week (every 3rd or 4th day) for 4 weeks (a total of eight times) via pulmonary delivery using the Microsprayer® Aerosolizer Pulmonary Aerosol-Kit for Mouse (Penn-Century Inc.). The control group was administered normal saline. D-Luciferin substrate (Regis Technologies Inc., IL, USA) was injected intraperitoneally at a dose of 150 mg/kg under anesthesia to attain a bioluminescence signal. The bioluminescence imaging after tumor inoculation was done on the 7th, 14th, 21st, 28th and 35th day using the IVIS® Lumina-XR system.

The body weight variation study was done by weekly body weight monitoring of the mice, throughout the investigation. The number of dead animals was recorded every day to plot the survival curve. GraphPad Prism 7 software (GraphPad Software Inc., La Jolla, CA, USA) was used to plot the survival curve of the mice bearing orthotopic lung-tumor implantation. Survival data of the mice were investigated by the Kaplan–Meier method using GraphPad Prism 7 software. This was followed by a log rank test for the comparison between different treatment groups.

Results and discussion

Synthesis of DSPE-PEG(2000)-MAL-T7

Firstly, DSPE-PEG(2000)-MAL-T7 conjugate was synthesized to formulate T7 targeted liposomes (T7-QR-lip). The conjugation reaction between Cys-T7 peptide and DSPE-PEG(2000)-MAL is a thiol-ene "click" reaction of the sulfhydryl group (–SH group) from the terminal cysteine of T7 peptide and the maleimide part of DSPE-PEG (2000)-MAL as shown in Figure 1B. The formation of DSPE-PEG(2000)-MAL-T7 was identified using MALDI-TOF-MS (Autoflex III; Bruker-Daltonics Inc.), as reported in previous studies.[16,21] The major peak of DSPE-PEG (2000)-MAL was observed at 2986.142 mass–charge ratio (m/z), which shifted right after conjugation. The major peak for DSPE- PEG(2000)-MAL-T7 was observed at 3936.438 (m/z) (see Figure 1C) and the peak was close to the theoretical calculated m/z of 3937.755. The peak for T7 (HAIYPRH) peptide with terminal cysteine was observed at m/z of 996.538. The theoretical calculated m/z was 996.150. The m/z values confirm the success of the conjugation reaction and illustrate that T7 peptide has been successfully conjugated to DSPE-PEG (2000)-MAL.

Formulation of T7 targeted liposomes

Both types of liposomes (T7 targeted liposomes and non-targeted liposomes) have been prepared by the film hydration method (Figure 1A), as described in the Methods section. T7 surface-functionalized liposomes have been formulated with

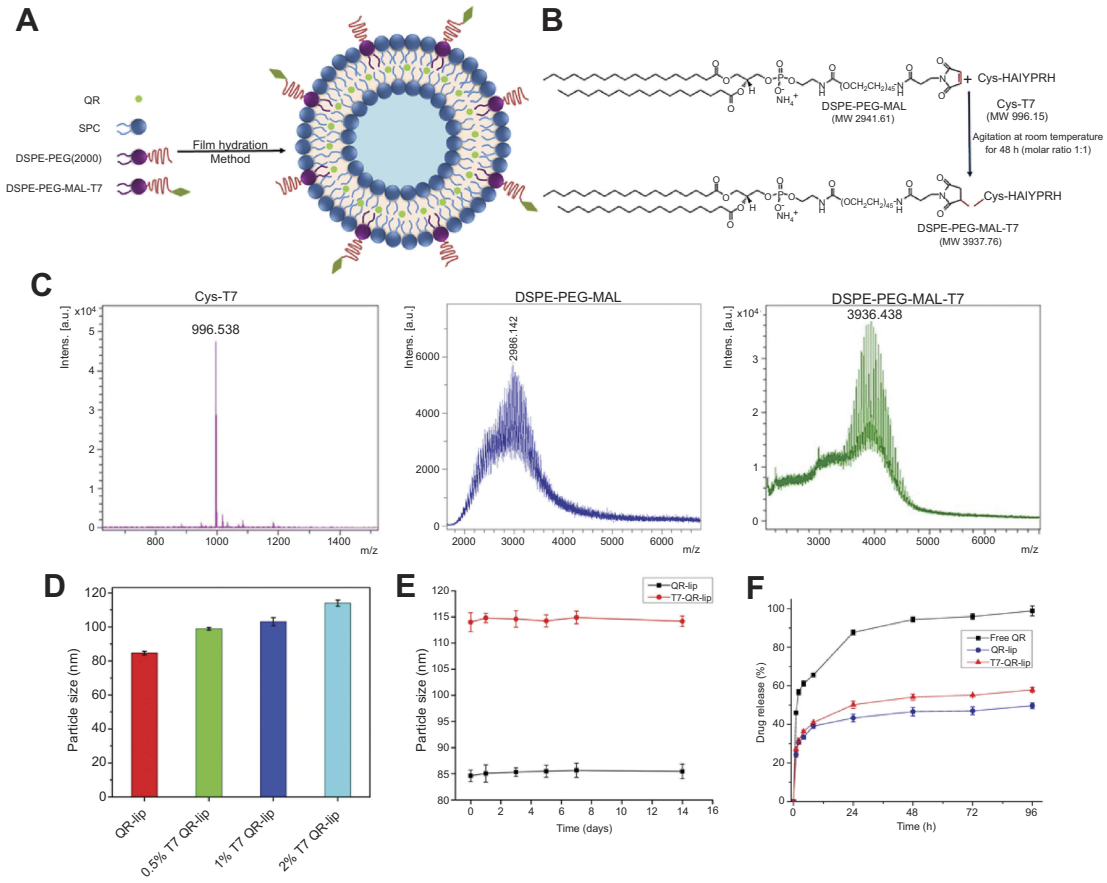

Figure 1 (**A**) Schematic Illustration of T7 targeted liposome formulation. (**B**) Synthesis of DSPE-PEG-MAL-T7 conjugate. (**C**) Matrix-assisted laser desorption/ionization–time of flight mass spectrometry spectra of Cys-T7, DSPE-PEG-MAL and DSPE-PEG-MAL-T7 conjugate. (**D**) Particle size of non-targeted QR-lip and T7-QR-lip after surface functionalization with different T7 peptide densities. (**E**) Stability study of 2% T7-QR-lip and QR-lip at 4 °C. Both types of liposomes showed no significant variation in particle size, demonstrating stability of the formulated liposomes. (**F**) In vitro release profiles of free QR, QR-lip and 2% T7-QR-lip for 96 h (n=3, mean±SD).
Abbreviations: lip, liposome; MW, molecular weight; m/z, mass–charge ratio; QR, quercetin; SPC, soybean lecithin.

different molar percentages ie, 0.5%, 1% and 2% of DSPE-PEG-MAL-T7 to lipid concentration in the liposomes using the film hydration method.

Characterization of liposomes: particle size, polydispersity index, encapsulation efficiency and stability study

The mean particle size of QR liposomal formulations (QR-lip and T7-QR-lip) ranged from 84 to 114 nm and the PDI was in a range of 0.097–0.22 (Table 1). The narrow PDI of the liposomal formulations indicates that the prepared liposomes have a uniform particle size distribution.[52] Moreover, surface functionalization of liposomes containing Cou6 and DiR with T7 peptide also resulted in an increase in particle size and PDI (Figure S1A–F). The appearance, particle-size distribution profile, particle size and PDI of various liposomes formulated in this study are shown in Figure S1A–F. The increased particle size of T7 targeted liposomes (T7-QR-lip) as compared to non-targeted liposomes (QR-lip) indicates that the

Table 1 Characterization of the formulated QR liposomes

Formulation	Mean diameter (nm)	Polydispersity	QR encapsulated (μg/ml)	Encapsulation efficiency (%)
QR-lip	84.63±1.10	0.092±0.007	573.90±2.55	95.48±0.047
0.5% T7-QR-lip	98.87±0.76	0.186±0.017	570.02±2.47	95.46±0.084
1% T7-QR-lip	103.1±2.40	0.176±0.043	559.12±2.74	95.37±0.124
2% T7-QR-lip	114.0±1.80	0.22±0.039	553.13±2.67	95.19±0.161

Note: n=3, mean±SD
Abbreviations: lip, liposome; QR, quercetin.

liposomes have been surface functionalized with T7 peptide with T7 anchors present on the liposomes' surface. Surface functionalization of the liposomes by increasing T7 peptide density ie, 0.5%, 1% and 2% resulted in a trend for increased particle size of liposomes. In a previous study, octreotide targeted liposomes loaded with doxorubicin were prepared with different ligands, ie, octreotide densities (0–4%), and showed an increase in the particle size of liposomes with the increase in ligand (octreotide density).[5353]

The liposomal formulations (T7-QR-lip and QR-lip) showed high encapsulation efficiency of about ~95% indicating that QR was well loaded in liposomes (Table 1). The particle size of non-targeted QR-lip and T7-QR-lip after surface functionalization with different T7 peptide densities is shown in Figure 1D. In the stability study, both types of liposomes (T7-QR-lip and QR-lip) showed no significant variation in particle size on storage at 4 °C, demonstrating stability of the liposomal formulations (Figure 1E).

In vitro drug release study

The in vitro drug release study was performed using dialysis method under sink conditions. Free QR solution showed a rapid release pattern with ~60% of QR release within 4 h in the release medium. T7-QR-lip and QR-lip showed sustained release of QR from 8 h to 96 h, as shown in Figure 1F. The total cumulative release of non-targeted QR-lip and T7-QR-lip was ~50% and 58% within 96 h, respectively. The results demonstrate that surface functionalization of liposomes with T7 peptide does not significantly influence the release profile of liposomes.

In vitro cytotoxicity study of T7 targeted liposomes by MTT assay

In vitro cytotoxicities of QR formulations were studied by MTT assay. The results are represented as cell viability plots (Figure 2A and B). The proliferation of cells was apparently suppressed in a dose-dependent manner, using different QR formulations. The in vitro cytotoxicity assay was performed on A549 cells and MRC-5 cells, using free QR solution, non-targeted QR liposomes (QR-lip) and T7 targeted QR liposomes (T7-QR-lip) at concentrations of 3.125, 6.25, 12.5, 25, 50 and 100 μM with an incubation period of 48 h. T7 targeted QR liposomes (T7-QR-lip) showed a trend for higher cytotoxicity by increasing T7 peptide density on the liposome surface in A549 cells, as compared to free QR and non-targeted QR liposomes (QR-lip). Further, at concentrations of 50 and 100 μM, 2% T7-QR-lip showed significantly higher cytotoxicity (~3-fold) as compared to free QR ($p<0.01$) against lung cancer cells (A549 cells). The IC50 values were calculated with GraphPad Prism 7 software for 2% T7-QR-lip (40.50±7.55 μM), QR-lip (63.54±9.02 μM) and free QR solution (107.46±7.62 μM). The difference in cytotoxicity can be attributed to surface functionalization of liposomes by T7 peptide, which enhanced the ability of liposomes to penetrate lung cancer (A549) cells by targeting TFR.[26,32] In this experiment, T7-QR-lip with different T7 peptide densities (0.5%, 1% and 2%) was used and the results have demonstrated that 2% T7 peptide density is optimum for anticancer activity.

In MRC-5 cells, no significant difference was observed in cytotoxicity caused by T7-QR-lip and QR-lip. However, QR-lip and T7-QR-lip showed relatively higher cytotoxicity as compared to free QR probably due to enhanced penetration ability of liposomes. These results are consistent with a previous study, in which TF targeted liposomes showed significantly lower cytotoxicity on non-cancer cell lines as compared to cancer cells.[54] Further, cell viability of A549 cells and MRC-5 cells incubated with T7-lip (without drug, ie blank) at different concentrations (ie 3.25–100 μM) for 48 h showed no cytotoxicity in both cell lines, demonstrating safety of the liposomes (Figure 4C).

In vitro cytotoxicity investigation of T7 targeted liposomes by apoptosis study

Apoptosis induction in the cancer cells is considered vital in cancer therapy and prevention.[55] In this experiment, apoptosis (cell death) of A549 cells was detected after treatment with T7-QR-lip, QR-lip and free QR solution at a QR concentration of 50 μM by FITC-Annexin V and PI double-staining and flow cytometry analysis. Annexin-V has high affinity for phosphatidylserine (PS), and readily binds to the PS translocated outside the cell membrane in the early stage of apoptosis. In late apoptosis, PI penetrates the ruptured cell membrane and stains the nuclei. Dual parametric dot-plots have been used to calculate the percentage of mechanically injured cells (Q1, Annexin-V– and PI+), late apoptotic cells (Q2, Annexin-V+ and PI+), viable (non-apoptotic) cells (Q3, Annexin-V– and PI–), and early apoptotic cells (Q4, Annexin-V+ and PI–).

Representative apoptosis plots of double-stained A549 cells are shown in Figure 3C. Quantitative data of A549

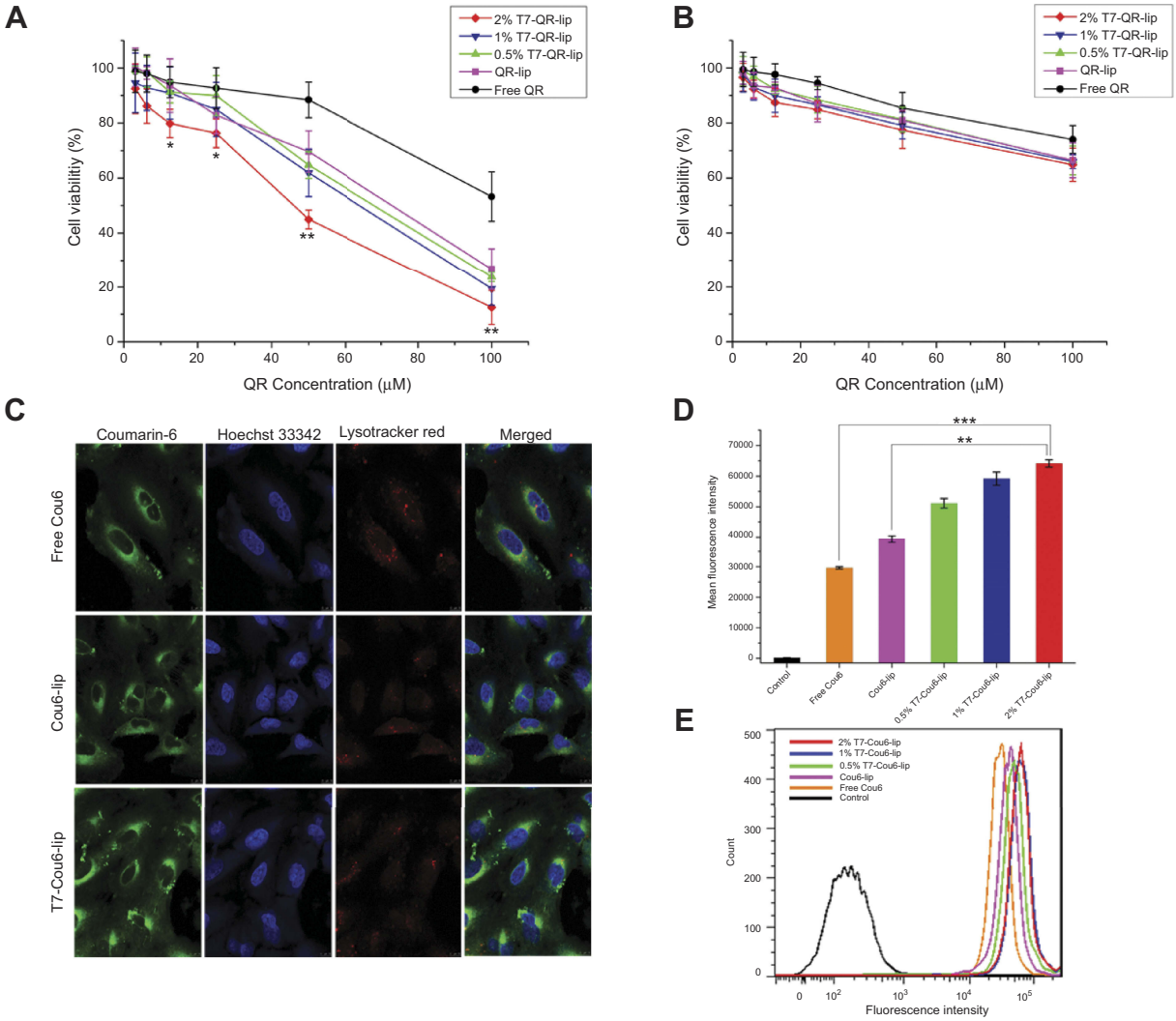

Figure 2 In vitro cytotoxicity of T7-QR-lip, non-targeted QR-lip and free QR solution against (**A**) A549 cells and (**B**) MRC cells assessed by MTT assay. Data are presented as mean±SD (n=3). $^{**}p<0.01$ compared with free QR group; $^{*}p<0.05$ compared with free QR group. (**C**) Cellular uptake of T7-Cou6-lip, Cou6-lip and free Cou6 in A549 cells by confocal laser scanning microscope. The scale bar represents 10 μm. (**D**) Mean fluorescence intensity of T7-Cou6-lip, Cou6-lip and free Cou6 after 3 h of treatment; control was untreated cells. Data are presented as mean±SD (n=3). $^{***}p<0.001$; $^{**}p<0.01$. (**E**) Quantitative analysis of T7-Cou6-lip, Cou6-lip and free Cou6 uptake by flow cytometry.
Abbreviations: Cou6, Coumarin-6; lip, liposome; MTT, 3-(4,5-dimethylthiazol-2-yl)-2,5-diphenyltetrazolium bromide; QR, quercetin.

cells for early apoptotic cells (Q4, Annexin-V+ and PI–) and late apoptotic cells (Q2, Annexin-V+ and PI+) attained by flow cytometry are shown in Figure 3D. T7-QR-lip have shown a higher induction of apoptosis than non-targeted liposomes (QR-lip) and free QR solution. Further, an increase in T7 peptide density on the liposome surface resulted in increased apoptosis induction (Figure 3C). This is probably due to the increased targeting of TFR on cancer cells by T7-QR-lip. The results of this experiment are consistent with a previous study, where QR induced apoptosis in A549 cells.[56] Moreover, the highest apoptosis was induced by T7-QR-lip with 2% T7 peptide density.

In vitro cytotoxicity study of T7 targeted liposomes by cell-cycle analysis study

The cell-cycle analysis study was done to gain deeper insight into the mechanism for the inhibitory effect on cell growth, and to determine the cell arrest phase. It has been shown by MTT assay that T7-QR-lip treatment of A549 cells resulted in higher proliferation inhibition than QR-lip (Figure 2A). To gain further insight into the inhibitory effects of liposomal QR, A549 cells were treated with QR and liposomal QR (T7-QR-lip and QR-lip) at a QR concentration of 50 μM for 24 h. After treatment of the cells with liposomal QR, cells were stained with PI and examined with flow cytometry. The cell-cycle profiles were analyzed by Modfit software.

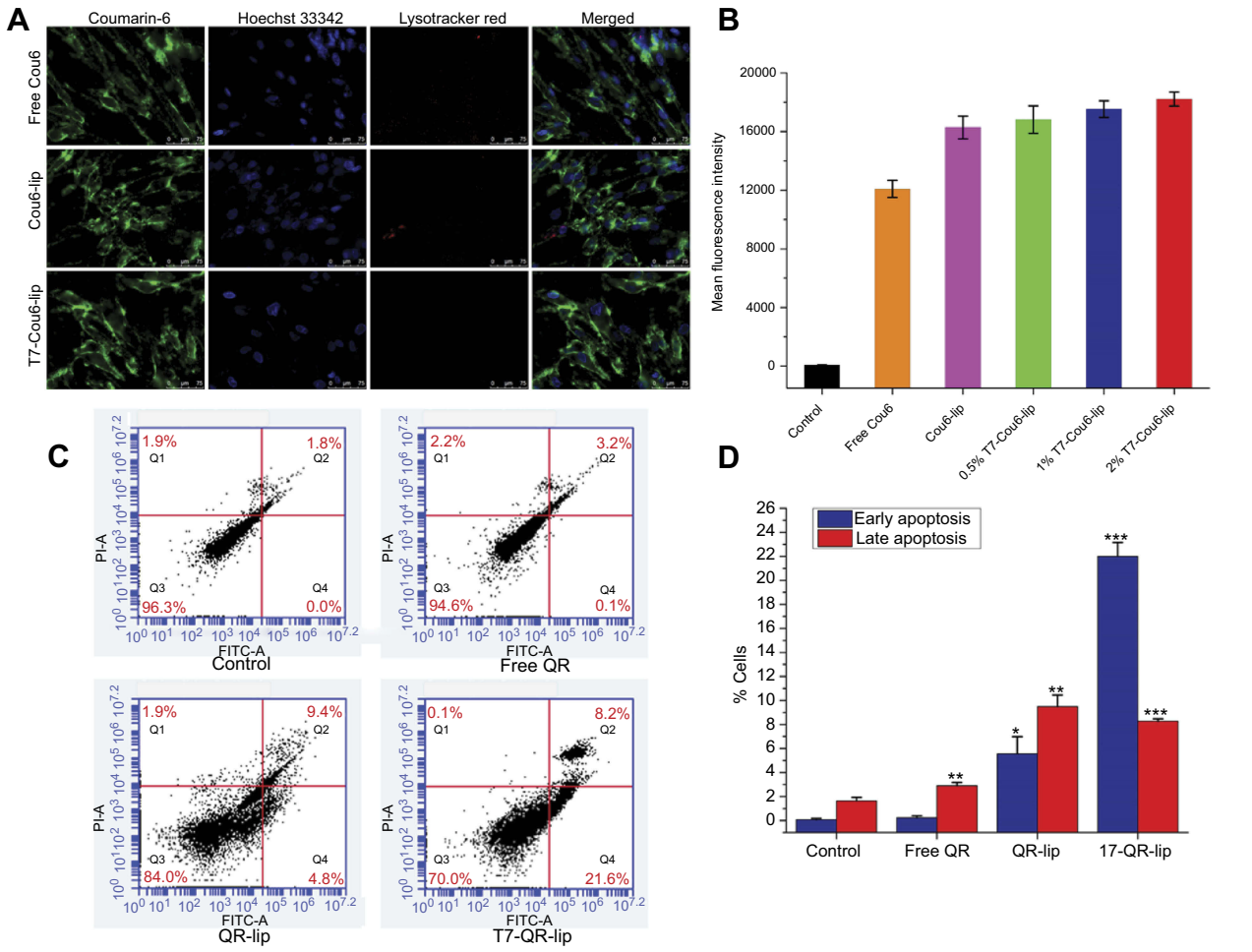

Figure 3 (**A**) Cellular uptake of T7-Cou6-lip, Cou6-lip and free Cou6 in MRC-5 (normal lung fibroblast) cells by confocal laser scanning microscope. The scale bar represents 75 µm. (**B**) Mean fluorescence intensity of T7-Cou6-lip, Cou6-lip and free Cou6 in MRC-5 cells after 3 h of treatment; control was untreated cells. Data are presented as mean±SD (n=3). (**C**) Apoptosis study on A549 cells by flow cytometry after treatment with different QR formulations at a QR concentration of 50 µM. (**D**) Quantitative data of A549 cells for early apoptotic cells (Q4, Annexin-V+ and PI–) and late apoptotic cells (Q2, Annexin-V+ and PI+) attained by flow cytometry. Data are presented as mean±SD (n=3). ***$p<0.001$ compared with control; **$p<0.01$ compared with control; *$p<0.05$ compared with control.
Abbreviations: Cou6, Coumarin-6; FITC, fluorescein isothiocyanate; lip, liposome; PI, propidium iodide; QR, quercetin.

The cell-cycle profiles suggest that higher S-phase cell-cycle arrest was observed for T7-QR-lip than for the QR-lip and free-QR treatment groups (Figure 4A and B). Further, the surface functionalization of liposomes with higher peptide density (2% T7 peptide) resulted in higher S-phase cell-cycle arrest in A549 cells. In a previous study, QR-mediated cell-cycle arrest and apoptosis in cancer cells have been reported.[38] The results of this experiment indicate that surface functionalization of liposomes with T7 peptide can significantly augment the QR inhibitory effect.

Cellular uptake study (in vitro target specificity) of T7 targeted liposomes

The cellular uptake of liposomes by A549 cancer cells has been studied by CLSM and flow cytometry.

Cellular uptake of liposomes (qualitative study) by CLSM

The cellular uptake (qualitative) study was performed on A549 and MRC-5 cells after 3-h incubation at 37 °C with T7 targeted Coumarin-6 liposomes (T7-Cou6-lip), Coumarin-6 liposomes (Cou-6 lip) and free Coumarin-6 (Cou-6) dye using the CLSM. After 3 h of incubation, T7-Cou6-lip treatment showed higher green fluorescence intensity in cytoplasm indicating higher cellular uptake in A549 cells as compared to the other treatment groups (Cou-6 lip and Cou-6 dye) (Figure 2C). However, in MRC-5 cells no difference was observed in green fluorescence intensity after treatment with T7-Cou6-lip and Cou-6 lip (Figure 3A and B). The higher cellular uptake in A549 cells was probably due to the surface

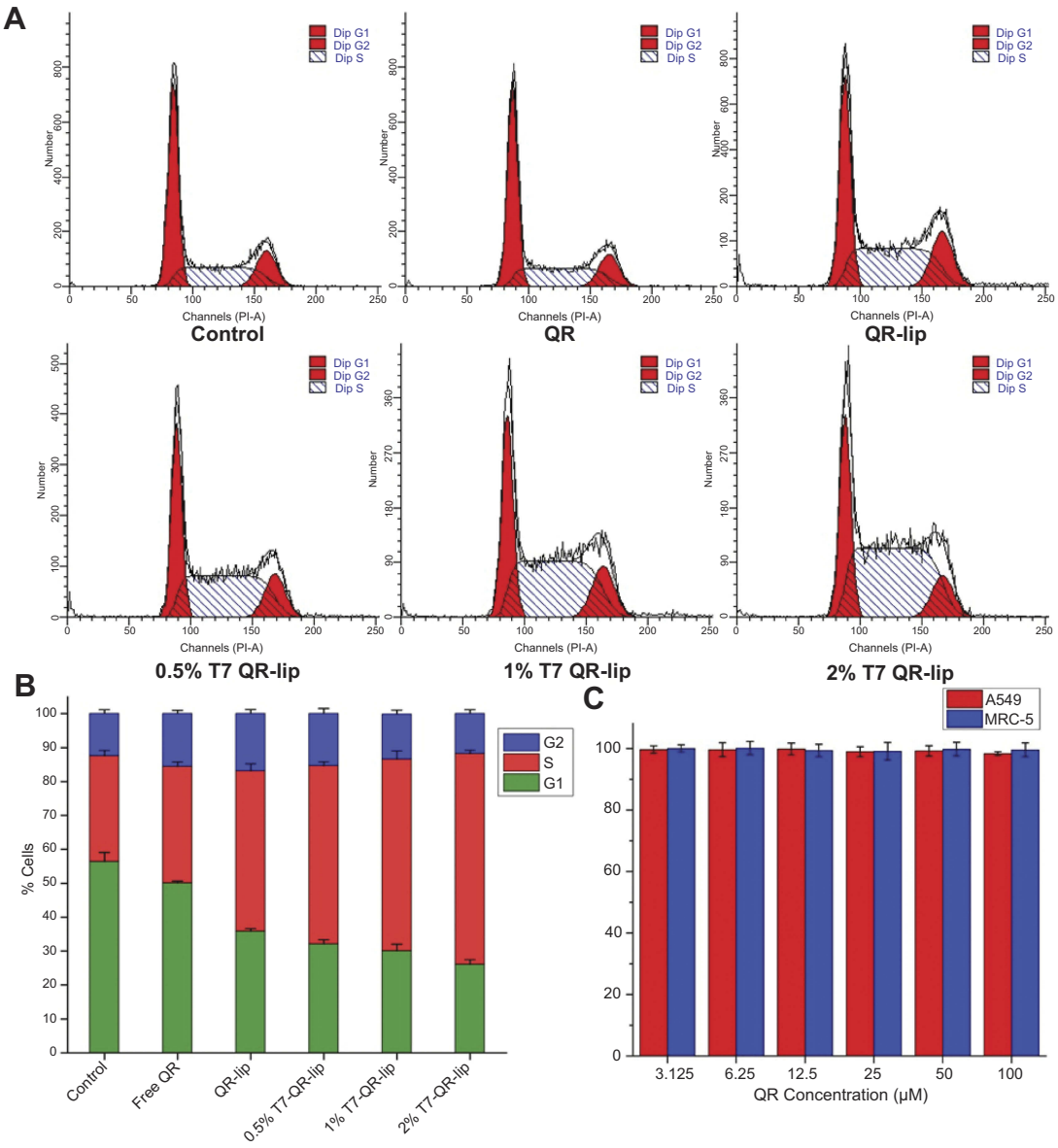

Figure 4 (**A**) Cell-cycle distribution in A549 cells, after treatment with T7-QR-lip, non-targeted QR-lip and free QR solution for 24 h at a QR concentration of 50 μM. (**B**) Stacked plot showing percentage of A549 cells in each phase of the cell cycle, after treatment with T7-QR-lip, non-targeted QR-lip and free QR solution. Data are presented as mean±SD (n=3). (**C**) Cell viability of A549 cells and MRC-5 cells incubated with T7-lip (without drug, ie blank) at different concentrations (3.25–100 μM) for 48 h. Data are presented as mean±SD (n=3).

Abbreviations: lip, liposome; PI, propidium iodide; QR, quercetin.

functionalization of liposomes with T7 peptide and the liposomes' functionalization enhances cellular uptake by specifically binding to TFR. Both A549 and MRC-5 cells were counterstained with Hoechst-33,342 to visualize the nuclei (blue fluorescence). Further, the internalization of T7-Cou6-lip and Cou6-lip was evaluated in lysosomes by staining A549 and MRC-5 cells with LysoTracker Red. A little red fluorescence was observed in the cells after treatment with T7-Cou6-lip and Cou6-lip, indicating that both types of liposomes have bypassed lysosomal degradation. These results are consistent with previous studies using liposomes, and indicate the liposomes' efficacy and prolonged duration of action in cancer therapy.[21,57]

Cellular uptake of liposomes (quantitative study) by flow cytometry

The quantitative measurement of cellular uptake of T7-Cou6-lip, Cou6-lip and Cou-6 dye in A549 and MRC-5 cells was done by flow cytometry. The intracellular mean fluorescence intensity increased significantly in A549 cells treated with 2%

T7-Cou6-lip (Figure 2D) compared to Cou6-lip ($p<0.01$) and Cou-6 dye ($p<0.001$). Further, the quantitative analysis of A549 cells treated with 2% T7-Cou6-lip showed a prominent right-shift in counts versus fluorescence intensity plot (cytometric analysis) than non-targeted Cou-6 lip (Figure 2E), suggesting enhanced cellular uptake of T7-Cou6-lip. Moreover, the increase in T7 peptide density on the liposome surface enhanced the cellular uptake and internalization of T7-Cou6-lip, while in MRC-5 cells no significant difference was observed in the intracellular mean fluorescence intensity of T7-Cou6-lip and Cou6-lip. The results of this experiment are in agreement with the qualitative cellular-uptake study and previous studies.[16,20,57,58]

Tumor-spheroid penetration and inhibition study

In vitro development of 3D lung tumor spheroids

The 3D lung tumor spheroids have been formed by the 2nd day (Figure S2A), after incubation of 1×10^3 A549 cells in each well of 96-well culture plates precoated with 80 µL of 2% (w/v) agarose in FBS-free medium at 37 °C, as previously reported.[49] The 3D lung tumor spheroids grew larger and denser with time during incubation in the subsequent days. Compact and uniform tumor spheroids (>300 µm) were selected for further use in 3D tumor-spheroid penetration and growth inhibition experiments (Figure S2B).

In vitro penetration study of Coumarin-6 liposomes in 3D lung tumor spheroids

Three-dimensional (3D) multicellular spheroids (in vitro) resemble more closely the in vivo microenvironment, as compared to a conventional monolayer culture system. The 3D tumor spheroids model possesses critical physiological parameters present in vivo such as complex multicellular structure, barriers to mass transport, etc. It has been suggested that 3D spheroids are appropriate in vitro models for drug penetration studies, compared to two-dimensional (2D) cell cultures.[59]

In this study, the penetration of liposomal formulations (T7-Cou6-lip, Cou-6 lip and free Cou6-dye) was investigated in 3D tumor spheroids of A549 cells by CLSM (Figure 5). The 3D tumor spheroids treated with free Cou-6 dye, non-targeted Cou6-lip and T7-Cou6-lip (2% T7 peptide density) showed fluorescence distributed in the core of tumor spheroids from the top to a depth of 48 µm, 72 µm and 120 µm, respectively. T7 surface-functionalized liposomes (T7-Cou6-lip) showed significantly deeper penetration and higher fluorescence intensity on a Z-projection image (Figure 5), as compared to other treatment groups (Cou6-lip and free Cou-6 dye). The results of this experiment clearly indicate that surface functionalization of liposomes with T7 peptide can improve the liposomes' ability to penetrate deeper into 3D tumor spheroids.

In vitro tumor growth inhibition study in 3D lung tumor spheroids

Uniform and compact tumor spheroids of >300 µm were selected for cytotoxic damage assay. In this study, 3D tumor spheroids were exposed to different treatment groups (2% T7-QR-lip, QR-lip and free QR) at 50 µM QR concentration for 5 days. Tumor spheroids were regularly imaged from 0 to 5 days using an inverted-phase microscope. Figure 6A represents the tumor-spheroid morphology changes after treatment with different formulations. As shown in Figure 6A, compact tumor spheroids with intact periphery were observed in the control group, while the tumor spheroids treated with free QR group retarded the growth of tumor spheroids as compared to the control group. In contrast, the tumor spheroids with a smeared rim and shedding of tumor-spheroid fragments were observed after treatment with Cou6-lip and T7-Cou6-lip. However, the tumor-spheroid growth inhibition was more pronounced in the case of T7-QR-Lip than non-targeted QR-lip.

As shown in Figure 6B, the tumor-spheroid volume ratio on the 5th day for the control group was 202.84±12.49%. After treatment with free QR, QR-lip and T7-QR-lip, the tumor-spheroid volume ratios on the 5th day were 131.43±10.68%, 112.40±8.21% and 87.62±4.12%, respectively. These results indicate that all QR formulations have retarded the tumor-spheroid growth. T7-QR-lip on the 5th day produced the most pronounced inhibition response as compared to the other treatment groups, ie control ($p<0.001$), free QR ($p<0.001$) and QR-lip ($p<0.001$). These results clearly suggest that T7-QR-lip may solve the problem of insufficient penetration and drug delivery to the inner core of 3D tumor spheroids.

In vivo therapeutic efficacy study of T7 targeted liposomes in orthotopic lung cancer mouse models

This involves the establishment of an A549-Luc orthotopic lung cancer mice model, a biodistribution study and a therapeutic efficacy study in mice bearing orthotopic lung-tumor implantation.

Establishment of an A549-Luc orthotopic lung cancer mice model

Firstly, an A549-luciferase (A549-Luc) orthotopic lung-tumor model was established in BALB/c nude mice. In

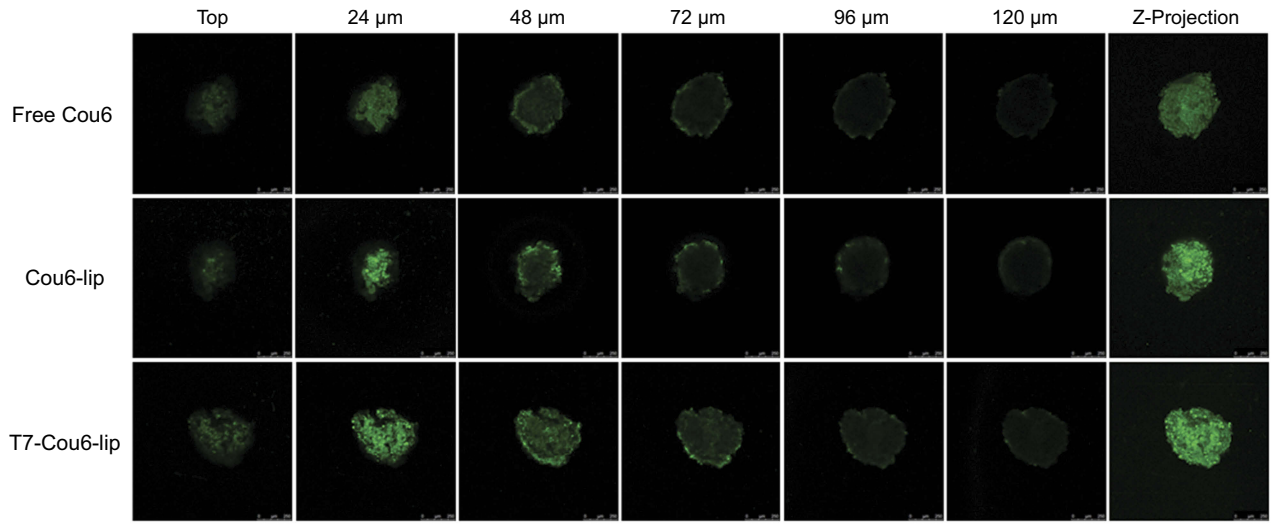

Figure 5 Confocal microscope images with a 24-µm interval between consecutive sections of three-dimensional multicellular tumor spheroids of A549 cells after incubation with free Cou6, Cou6-lip and T7-Cou6-lip, at a Cou6 concentration of 0.5 µg/ml for 24 h. The scale bar represents 250 µm.
Abbreviations: Cou6, Coumarin-6; lip, liposomes.

the orthotopic lung cancer model, the tumor grows in the microenvironment of the lungs. Thus, the orthotopic lung cancer model is clinically more relevant in the treatment of lung cancer than ectopic tumor models created by the subcutaneous inoculation of human lung cancer cells into mice.[20] In order to prevent the metastasis of cancer cells to other organs, Matrigel Matrix was used during orthotopic lung-tumor implantation to anchor the cancer cells at the tumor site.

Intrathoracic injection of A549-Luc cells to establish an orthotopic lung tumor model in mice is shown in Figure S3A. The orthotopic lung tumor-bearing mouse was dissected and solid tumor was observed on the lungs (Figure S3B). Further, the lungs harvested from the orthotopic lung tumor-bearing mouse showed solid tumor on the lungs surrounded by normal lung tissue (Figure S3C). Figure 7A shows a bioluminescence image of an A549-luciferase orthotopic lung tumor-bearing mouse, after tumor model establishment. Further, the lung position was confirmed using an X-ray and bioluminescence overlayed image as shown in Figure 7A.

Biodistribution of T7 targeted liposomes in vivo through pulmonary delivery

A biodistribution study was done in BALB/c nude mice with orthotopic lung-tumor implantation via pulmonary delivery of T7 targeted DiR liposomes (T7-DiR-lip) by the Microsprayer® Aerosolizer Pulmonary Aerosol-Kit for Mouse (Penn-Century Inc.), as shown in Figure S4A–C. The successful establishment of an A549-Luc orthotopic lung-tumor model in the mouse was confirmed by bioluminescent imaging on the 7th day after A549-Luc cell inoculation using the IVIS® Lumina-XR system (Figure 7A). In the biodistribution study, the liposomes were administered via pulmonary delivery to minimize the toxicity to other organs. Administration of therapeutic agents through the inhalation route has been considered better for the accumulation of drugs in the lungs with low systemic toxicity.[60] Liposomes containing triptolide have been shown to be effective in the inhibition of lung cancer when administered via the pulmonary route.[20]

T7-DiR-lip were mainly concentrated in the lungs after pulmonary administration, as shown in Figure 7B. Fluorescent images of the mice at different time points are shown in Figure 7B. The fluorescent images show that T7-QR-lip were accumulated and retained, mainly in the lungs, and fluorescence can be visualized at approximately the same level for 72 h. Further, fluorescence in the lungs can be even visualized at 96 h. These results could support the potential application of T7 targeted liposomes, as an extended (sustained) release delivery system for targeting the lung-tumor site. In a previous study, lung-specific localization of liposomes was observed after endotracheal administration of the liposomes.[20]

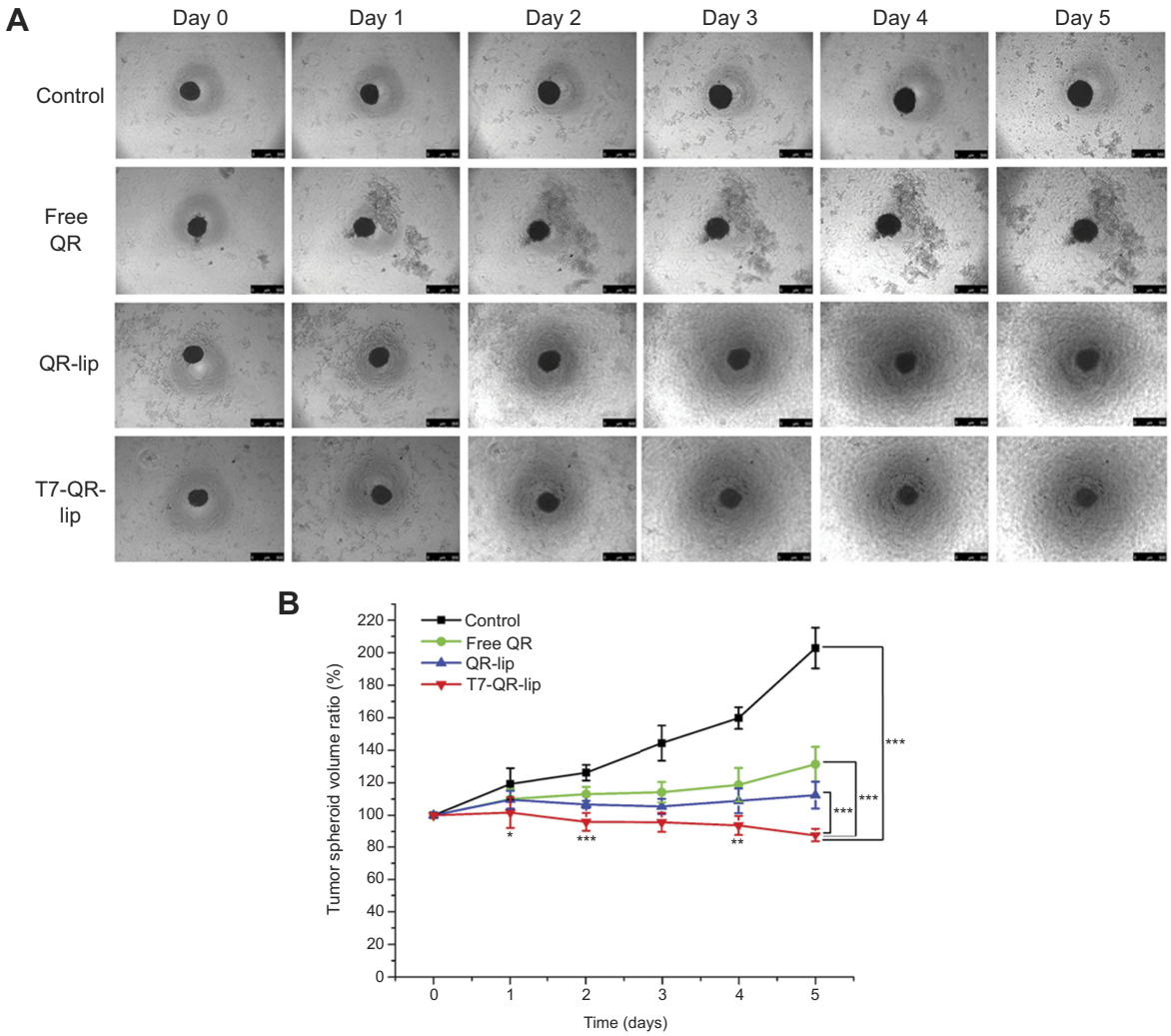

Figure 6 (**A**) Representative bright-field images of A549 tumor spheroids after treatment with T7-QR-lip, non-targeted QR-lip and free QR solution at a concentration of 50 μM. The scale bar represents 500 μm. (**B**) Time-related volume of A549 multicellular tumor spheroids after treatment with T7-QR-lip, non-targeted QR-lip and free QR solution at a concentration of 50 μM from 0 to 5 days. Data are presented as mean±SD (n=5). ***p<0.001 compared with free QR group; **p<0.01 compared with free QR group; *p<0.05 compared with free QR group.
Abbreviations: lip, liposome; QR, quercetin.

Therapeutic efficacy of T7 targeted liposomes through pulmonary delivery in mice bearing A549-Luc orthotropic implantation

Seven days after orthotopic lung-tumor implantation, mice were randomized into control and treatment groups. The fluorescence imaging data in the biodistribution study of T7-DiR-lip have shown that fluorescence can be observed on the lungs even after 96 h of pulmonary administration (Figure 7B). The mice in treatment groups received free QR solution, QR-lip and T7-QR-lip at a QR dose of 10 mg/kg twice a week (every 3rd or 4th day) via pulmonary delivery (a total of 8 doses, as shown in Figure 8A) and the bioluminescence imaging of orthotopic lung tumor-bearing BALB/c nude mice was done in vivo on the 7th, 14th, 21st, 28th and 35th day by the IVIS Lumina-XR system (Figure 8B). The mice were intraperitoneally injected with D-luciferin substrate (Regis Technologies Inc.) under anesthesia at a dose of 150 mg/kg, to attain the bioluminescent signal from the lung tumor.

In the present study, we monitored the variations in bioluminescence signals of the lung tumor to evaluate the anticancer efficacy of QR formulations in mice with orthotopic lung-tumor implantation (Figure 8C). Rapid tumor growth was observed in the saline group in the entire experiment period. However, tumor growth inhibition was observed in groups treated with free-QR, non-targeted QR-lip and targeted T7-QR-lip as compared to the saline group. The mice group receiving T7-QR-lip

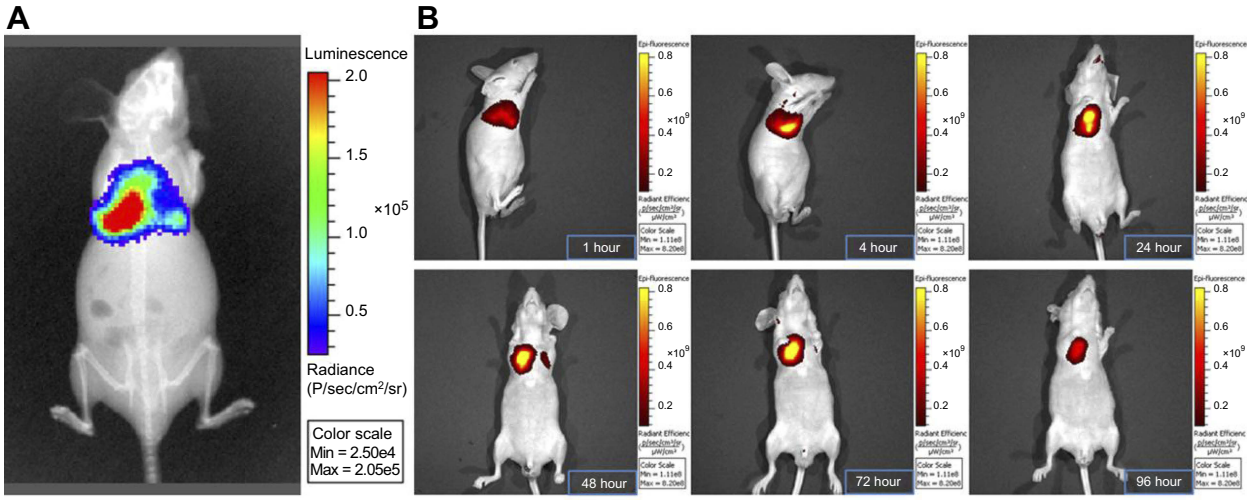

Figure 7 Biodistribution of T7 targeted liposomes in an orthotopic lung tumor-bearing mouse after endotracheal administration. (**A**) Bioluminescence image of an A549-luciferase orthotopic lung tumor-bearing mouse, after tumor model establishment. (**B**) Biodistribution behavior of T7 targeted 1,1'-dioctadecyltetramethyl-indotricarbocyanine iodide liposomes by fluorescent imaging in an A549-luciferase orthotopic lung tumor-bearing mouse at different time points.

showed the strongest tumor growth inhibition after receiving 8 doses through pulmonary administration, as compared to non-targeted QR-lip, free-QR and the saline groups. On the 35th day, mice in the T7-QR-lip group showed significantly lower bioluminescence signal intensity ($p<0.05$) compared with mice treated with saline (control group) (Figure 8C). These results indicate that surface functionalization of the liposomes with T7 peptide can contribute to enhanced therapeutic efficacy of the liposomes in lung cancer therapy.

A body weight variation study was done in lung tumor-bearing mice. The body weights of tumor-bearing mice during treatment were monitored weekly throughout the investigation. A change in body weight of the tumor-bearing mice during treatment has been suggested as a marker of toxicity.[20] In the present study, no significant weight variations were observed in all treatment groups as compared to the saline group, indicating no toxicity of QR formulations administered through pulmonary delivery (Figure 8D). This demonstrates that the pulmonary administration of anticancer drug (QR-loaded liposomes) can be a well-tolerated strategy for the inhibition of tumor growth and for lung cancer therapy. In a previous study, no significant body weight variations were observed while using targeted liposomes for lung cancer treatment via pulmonary administration in mice.[20]

The number of dead animals was recorded every day to create the survival curve (Figure 8E). The lifespan of mice treated with T7-QR-lip was significantly prolonged ($p=0.0018$ compared with saline), with a median survival time of 69 days. The median survival time of the mice treated with T7-QR-lip (69 days), QR-lip (57 days) and free-QR (48 days) was 1.68-fold, 1.39-fold and 1.17-fold longer, respectively, than the survival time (41 days) of the control group.

The results of the in vivo therapeutic efficacy study (tumor growth inhibition, no significant body weight variation of treated mice and the survival curve) show safety and efficacy of T7-QR-lip after pulmonary administration in lung cancer therapy of orthotopic lung tumor-bearing mice. The enhanced anticancer efficacy of T7-QR-lip can be attributed to the specific characteristics of surface-functionalized liposomes (prolonged circulation time due to PEGylation,[61] high drug accumulation in the lungs via pulmonary administration and delayed lung clearance[62,63]) and active targeting of over-expressed receptors ie, TFR at the tumor site[64–66], thus contributing to the anticancer activity of QR and showing promise in lung cancer therapy.

Conclusions

In this study, T7 surface-functionalized liposomes with different T7 peptide densities (0.5%, 1% and 2%) and non-targeted QR-loaded liposomes were successfully formulated having encapsulation efficiency of ~95%. Anticancer activity of formulated liposomes was investigated in lung cancer ie, A549 cells and normal lung ie, MRC-5 cells using the formulated liposomes. T7 surface-functionalized liposomes (2% T7-QR-lip) demonstrated significantly enhanced cytotoxicity, cellular uptake, S-phase cell-cycle arrest and apoptosis in A549 cells as compared to non-targeted QR-lip due to receptor-mediated endocytosis. However, in MRC-5 cells no significant variation

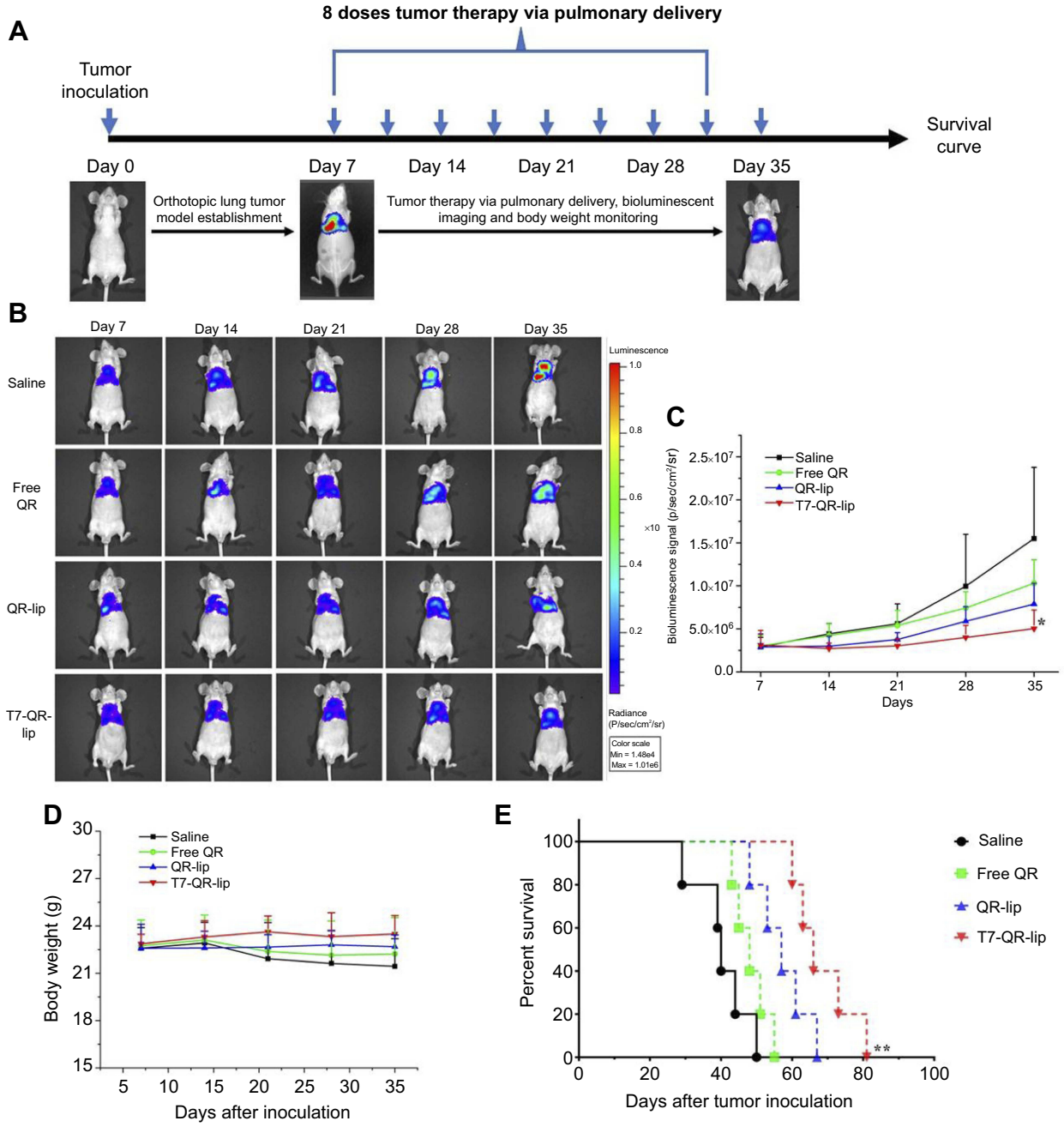

Figure 8 Therapeutic efficacy of T7-QR-lip after pulmonary administration in BALB/c nude mice with orthotopic lung-tumor implantation. (**A**) Treatment schedule of QR formulations in orthotopic A549-Luc tumor-bearing mice (**B**) Representative images of bioluminescence changes in mice during treatment with different QR formulations (ie, T7-QR-lip, non-targeted QR-lip and free QR solution) and saline as a control (n=5) using the IVIS® Lumina-XR system. (**C**) Changes in bioluminescence signal monitored by the IVIS® Lumina-XR system (n=5) during treatment with different QR formulations; *p<0.05, compared with saline. (**D**) Body weight variations of orthotopic lung tumor-bearing mice in different treatment groups during therapy. (**E**) Survival curve of mice with orthotopic lung-tumor implantation after pulmonary administration of different QR formulations; **p<0.01, compared with saline.

Abbreviations: lip, liposome; QR, quercetin.

was observed in T7-QR-lip and QR-lip in cytotoxicity and cellular uptake studies. Further, 2% T7-Cou6-lip showed significantly deeper penetration in 3D lung tumor spheroids. The 2% T7-QR-lip showed the most pronounced inhibition response on growth of 3D lung tumor spheroids, as compared to the other treatment groups. The biodistribution studies exhibited that T7 surface-functionalized liposomes mainly concentrated in the lungs following their pulmonary administration. Further, the mice with orthotopic lung-tumor implantation receiving T7-QR-lip through pulmonary administration showed the strongest tumor growth inhibition and survival time without any systemic toxicity as compared to the other

treatment groups (non-targeted QR-lip and free-QR). Both in vitro and in vivo results of this study suggest that T7 surface-functionalized liposomes are a promising nanocarrier for lung cancer therapy by receptor-mediated targeting at the tumor site.

Acknowledgments

This work was supported by Hong Kong Baptist University Special Development Fund (SDF18-0319-P03) and Faculty Research Grant (FRG2/16-17/073 and FRG2/15-16/078), grant of the Science and Technology Planning Project of Guangdong Province (2017A050506027) and grant of the Science and Technology Program of Guangzhou (201807010053).

Disclosure

The authors report no conflicts of interest in this work.

References

1. World Health Organization. 2018. Cancer fact sheet 2018, the global cancer observatory. Available from: http://gco.iarc.fr/today/data/factsheets/cancers/39-All-cancers-fact-sheet.pdf. Accessed August 15, 2018
2. Siegel RL, Miller KD, Jemal A. Cancer Statistics, 2018. *CA Cancer J Clin*. 2018;67(1):7–30. doi:10.3322/caac.21387
3. American Cancer Society Surveillance Research. Estimated deaths for the four major cancers by sex and age group. Available from: https://www.cancer.org/content/dam/cancer-org/research/cancer-facts-and-statistics/annual-cancer-facts-and-figures/2016/estimated-deaths-for-the-four-major-cancers-by-sex-and-age-group-2016.pdf. Published 2016. Accessed July 13, 2018.
4. Ramalingam SS, Owonikoko TK, Khuri FR. Lung cancer: new biological insights and recent therapeutic advances. *CA Cancer J Clin*. 2011;61(2):91–112. doi:10.3322/caac.20102
5. MacManus M, Everitt S, Schimek-Jasch T, Li XA, Nestle U, Kong F-M. (Spring). Translational lung cancer research. *Transl Lung Cancer Res*. 2017;6(6):670–688. Available from: http://tlcr.amegroups.com/article/view/16034/12985. Accessed September 22, 2018.
6. Dobson Amato KA, Hyland A, Reed R, et al. Tobacco cessation may improve lung cancer patient survival. *J Thorac Oncol*. 2015;10(7):1014–1019. doi:10.1097/JTO.0000000000000578
7. Maeda H, Nakamura H, Fang J. The EPR effect for macromolecular drug delivery to solid tumors: improvement of tumor uptake, lowering of systemic toxicity, and distinct tumor imaging in vivo. *Adv Drug Deliv Rev*. 2013;65(1):71–79. doi:10.1016/J.ADDR.2012.10.002
8. Calixto G, Fonseca-Santos B, Chorilli M, Bernegossi J. Nanotechnology-based drug delivery systems for treatment of oral cancer: a review. *Int J Nanomedicine*. 2014;9(1):3719. doi:10.2147/IJN.S61670
9. Ruiz ME, Gantner ME, Talevi A. Applications of nanosystems to anticancer drug therapy (Part II. Dendrimers, micelles, lipid-based nanosystems). *Recent Pat Anticancer Drug Discov*. 2014;9(1):99–128. Available from: http://www.ingentaconnect.com/content/ben/pra/2015/00000010/00000001%5Cnhttp://www.ncbi.nlm.nih.gov/pubmed/23578193.
10. Drbohlavova J, Chomoucka J, Adam V, et al. Nanocarriers for anticancer drugs–new trends in nanomedicine. *Curr Drug Metab*. 2013;14(5):547–564.
11. Pattni BS, Chupin VV, Torchilin VP. New developments in liposomal drug delivery. *Chem Rev*. 2015;115(19):10938–10966. doi:10.1021/acs.chemrev.5b00046
12. Danhier F, Préat V. Strategies to improve the EPR effect for the delivery of anti-cancer nanomedicines. *Cancer Cell Microenviron*. 2015;2(3):1–7. doi:10.14800/ccm.808
13. Garbuzenko OB, Saad M, Pozharov VP, Reuhl KR, Mainelis G, Minko T. Inhibition of lung tumor growth by complex pulmonary delivery of drugs with oligonucleotides as suppressors of cellular resistance. *Proc Natl Acad Sci U S A*. 2010;107(23):10737–10742. doi:10.1073/pnas.1004604107
14. Lim SB, Banerjee A, Önyüksel H. Improvement of drug safety by the use of lipid-based nanocarriers. *J Control Release*. 2012;163(1):34–45. doi:10.1016/j.jconrel.2012.06.002
15. Deshpande PP, Biswas S, Torchilin VP. Current trends in the use of liposomes for tumor targeting. *Nanomedicine (Lond)*. 2014;8(9):1–32. doi:10.2217/nnm.13.118.Current
16. Lin C, Zhang X, Chen H, et al. Dual-ligand modified liposomes provide effective local targeted delivery of lung-cancer drug by antibody and tumor lineage-homing cell-penetrating peptide. *Drug Deliv*. 2018;25(1):256–266. doi:10.1080/10717544.2018.1425777
17. Dicheva BM, Ten Hagen TLM, Schipper D, et al. Targeted and heat-triggered doxorubicin delivery to tumors by dual targeted cationic thermosensitive liposomes. *J Control Release*. 2014;195:37–48. doi:10.1016/J.JCONREL.2014.07.058
18. Al-Ahmady ZS, Chaloin O, Kostarelos K. Monoclonal antibody-targeted, temperature-sensitive liposomes: in vivo tumor chemotherapeutics in combination with mild hyperthermia. *J Control Release*. 2014;196:332–343. doi:10.1016/J.JCONREL.2014.10.013
19. Chi B, Wong K, Qin L, et al. Carbonic anhydrase IX-directed immunoliposomes for targeted drug delivery to human lung cancer cells in vitro. *Dovepress*. 2014;8:993–1001.
20. Lin C, Wong BCK, Chen H, et al. Pulmonary delivery of triptolide-loaded liposomes decorated with anti-carbonic anhydrase IX antibody for lung cancer therapy. *Sci Rep*. 2017;7(1):1097. doi:10.1038/s41598-017-00957-4
21. Zhang X, Lin C, Lu A, et al. Liposomes equipped with cell penetrating peptide BR2 enhances chemotherapeutic effects of cantharidin against hepatocellular carcinoma. *Drug Deliv*. 2017;24(1):986–998. doi:10.1080/10717544.2017.1340361
22. She Z, Zhang T, Wang X, et al. The anticancer efficacy of pixantrone-loaded liposomes decorated with sialic acid–octadecylamine conjugate. *Biomaterials*. 2014;35(19):5216–5225. doi:10.1016/J.BIOMATERIALS.2014.03.022
23. Torchilin VP. Passive and active drug targeting: drug delivery to tumors as an example. In: Schafer-Korting M, editor. *Handbook of Experimental Pharmacology*. Berlin, Germany: Springer; Vol. 7. 2010;3–53. doi: 10.1007/978-3-642-00477-3
24. Riaz MK, Riaz MA, Zhang X, et al. Surface functionalization and targeting strategies of liposomes in solid tumor therapy: A review. *Int J Mol Sci*. 2018;19:1. doi:10.3390/ijms19010195
25. Riaz MK, Tyagi D, Yang Z. Surface engineering: incorporation of bioactive compound. In: Yan B, Zhou H, Gardea-Torresdey JL, editors. *Bioactivity of Engineered Nanoparticles*. Singapore: Springer Nature; 2017:111–143. doi:10.1007/978-981-10-5864-6_6
26. Han L, Huang R, Liu S, Huang S, Jiang C. Peptide-conjugated PAMAM for targeted doxorubicin delivery to transferrin receptor overexpressed tumors. *Mol Pharm*. 2010;7(6):2156–2165. doi:10.1021/mp100185f
27. Singh M. Transferrin as a targeting ligand for liposomes and anticancer drugs. *Curr Pharm Des*. 1999;6:443–451.
28. Daniels TR, Bernabeu E, Rodríguez JA, et al. The transferrin receptor and the targeted delivery of therapeutic agents against cancer. *Biochim Biophys Acta*. 2012;1820(3):291–317. doi:10.1016/j.bbagen.2011.07.016
29. Wang J, Pantopoulos K. Regulation of cellular iron metabolism. *Biochem J*. 2011;434(3):365–381. doi:10.1042/BJ20101825

30. Anabousi S, Bakowsky U, Schneider M, Huwer H, Lehr CM, Ehrhardt C. In vitro assessment of transferrin-conjugated liposomes as drug delivery systems for inhalation therapy of lung cancer. *Eur J Pharm Sci*. 2006;29(5):367–374. doi:10.1016/j.ejps.2006.07.004
31. Zhai G, Wu J, Yu B, Guo C, Yang X, Lee RJ. A transferrin receptor-targeted liposomal formulation for docetaxel. *J Nanosci Nanotechnol*. 2010;10(8):5129–5136. doi:10.1166/jnn.2010.2393
32. Lee JH, Engler JA, Collawn JF, Moore BA. Receptor mediated uptake of peptides that bind the human transferrin receptor. *Eur J Biochem*. 2001;268(7):2004–2012. doi:10.1046/j.1432-1327.2001.02073.x
33. Wang Z, Zhao Y, Jiang Y, et al. Enhanced anti-ischemic stroke of ZL006 by T7-conjugated PEGylated liposomes drug delivery system. *Sci Rep*. 2015;5:12651. doi:10.1038/srep12651
34. Oh S, Kim BJ, Singh NP, Lai H, Sasaki T. Synthesis and anti-cancer activity of covalent conjugates of artemisinin and a transferrin-receptor targeting peptide. *Cancer Lett*. 2009;274 (1):33–39. doi:10.1016/j.canlet.2008.08.031
35. Wu H, Yao L, Mei J, Li F. Development of synthetic of peptide-functionalized liposome for enhanced targeted ovarian carcinoma therapy. *Int J Clin Exp Med*. 2014;7(12):4809–4818.
36. Zong T, Mei L, Gao H, et al. Synergistic dual-ligand doxorubicin liposomes improve targeting and therapeutic efficacy of brain glioma in animals. *Mol Pharm*. 2014;11(7):2346–2357. doi:10.1021/mp500057n
37. Zhang Y, Zhai M, Chen Z, et al. Dual-modified liposome codelivery of doxorubicin and vincristine improve targeting and therapeutic efficacy of glioma. *Drug Deliv*. 2017;24(1):1045–1055. doi:10.1080/10717544.2017.1344334
38. Srivastava S, Somasagara RR, Hegde M, et al. Quercetin, a natural flavonoid interacts with DNA, arrests cell cycle and causes tumor regression by activating mitochondrial pathway of apoptosis. *Sci Rep*. 2016;6:24049. doi:10.1038/srep24049
39. Lu J, L V P, Fang J, Rodriguez-Nieto S, Zhivotovsky B, Holmgren A. Inhibition of mammalian thioredoxin reductase by some flavonoids: implications for myricetin and quercetin anticancer activity. *Cancer Res*. 2006;66(8):4410–4418. doi:10.1158/0008-5472.CAN-05-3310
40. Del Follo-Martinez A, Banerjee N, Li X, Safe S, Mertens-Talcott S. Resveratrol and quercetin in combination have anticancer activity in colon cancer cells and repress oncogenic microRNA-27a. *Nutr Cancer*. 2013;65(3):494–504. doi:10.1080/01635581.2012.725194
41. Formica JV, Regelson W. Review of the biology of quercetin and related bioflavonoids. *Food Chem Toxicol*. 1995;33(12):1061–1080. doi:10.1016/0278-6915(95)00077-1
42. Nguyen TTT, Tran E, Nguyen TH, Do PT, Huynh TH, Huynh H. The role of activated MEK-ERK pathway in quercetin-induced growth inhibition and apoptosis in A549 lung cancer cells. *Carcinogenesis*. 2003;25(5):647–659. doi:10.1093/carcin/bgh052
43. Xingyu Z, Peijie M, Dan P, et al. Quercetin suppresses lung cancer growth by targeting Aurora B kinase. *Cancer Med*. 2016;5 (11):3156–3165. doi:10.1002/cam4.891
44. Suntres ZE. Liposomal antioxidants for protection against oxidant-induced damage. *J Toxicol*. 2011;2011:152474. doi:10.1155/2011/152474
45. Lamson DW, Brignall MS. Antioxidants and cancer, part 3: quercetin. *Altern Med Rev*. 2000;5(3):196–208. Available from: http://www.ncbi.nlm.nih.gov/pubmed/10869101
46. Kashyap D, Mittal S, Sak K, Singhal P, Tuli HS. Molecular mechanisms of action of quercetin in cancer: recent advances. *Tumor Biol*. 2016;37(10):12927–12939. doi:10.1007/s13277-016-5184-x
47. Chou -C-C, Yang J-S, Lu H-F, et al. Quercetin-mediated cell cycle arrest and apoptosis involving activation of a caspase cascade through the mitochondrial pathway in human breast cancer MCF-7 cells. *Arch Pharm Res*. 2010;33(8):1181–1191. doi:10.1007/s12272-010-0808-y
48. Gang W, Jie WJ, Ping ZL, et al. Liposomal quercetin: evaluating drug delivery *in vitro* and biodistribution *in vivo*. *Expert Opin Drug Deliv*. 2012;9(6):599–613. doi:10.1517/17425247.2012.679926
49. Zhang Q, Tang J, Fu L, et al. A pH-responsive α-helical cell penetrating peptide-mediated liposomal delivery system. *Biomaterials*. 2013;34(32):7980–7993. doi:10.1016/J.BIOMATERIALS.2013.07.014
50. Liang D-S, Su H-T, Liu Y-J, Wang A-T, Qi X-R. Tumor-specific penetrating peptides-functionalized hyaluronic acid-d-α-tocopheryl succinate based nanoparticles for multi-task delivery to invasive cancers. *Biomaterials*. 2015;71:11–23. doi:10.1016/J.BIOMATERIALS.2015.08.035
51. Onn A, Isobe T, Itasaka S, et al. Development of an orthotopic model to study the biology and therapy of primary human lung cancer in nude mice. *Clin Cancer Res*. 2003;9:5532–5539.
52. Danaei M, Dehghankhold M, Ataei S, et al. Impact of particle size and polydispersity index on the clinical applications of lipidic nanocarrier systems. *pharmaceutics*. 2018;10(2):57. doi:10.3390/pharmaceutics10020057
53. Li H, Yuan D, Sun M, Ping Q. Effect of ligand density and PEG modification on octreotide-targeted liposome via somatostatin receptor *in vitro* and *in vivo*. *Drug Deliv*. 2016;23(9):3562–3572. doi:10.1080/10717544.2016.1209797
54. Deshpande P, Jhaveri A, Pattni B, Biswas S, Torchilin VP. Transferrin and octaarginine modified dual-functional liposomes with improved cancer cell targeting and enhanced intracellular delivery for the treatment of ovarian cancer. *Drug Deliv*. 2018;25(1):517–532. doi:10.1080/10717544.2018.1435747
55. Ichim G, Tait SWG. A fate worse than death: apoptosis as an oncogenic process. *Nat Rev Cancer*. 2016;16(8):539–548. doi:10.1038/nrc.2016.58
56. Nguyen TTT, Tran E, Nguyen TH, Do PT, Huynh TH, Huynh H. The role of activated MEK-ERK pathway in quercetin-induced growth inhibition and apoptosis in A549 lung cancer cells. *Carcinogenesis*. 2004;25(5):647–659. doi:10.1093/carcin/bgh052
57. Jhaveri A, Deshpande P, Pattni B, Torchilin V. Transferrin-targeted, resveratrol-loaded liposomes for the treatment of glioblastoma. *J Control Release*. 2018;277(November2017):89–101. doi:10.1016/j.jconrel.2018.03.006
58. Liu Y, Ran R, Chen J, et al. Paclitaxel loaded liposomes decorated with a multifunctional tandem peptide for glioma targeting. *Biomaterials*. 2014;35(17):4835–4847. doi:10.1016/J.BIOMATERIALS.2014.02.031
59. Mehta G, Hsiao YA, Ingram M, et al. Opportunities and challenges for use of tumor spheroids as models to test drug delivery and efficacy. *J Control Release*. 2012;164(2):192–204. doi:10.1016/j.jconrel.2012.04.045.Opportunities
60. Luo T, Loira-Pastoriza C, Patil HP, et al. PEGylation of paclitaxel largely improves its safety and anti-tumor efficacy following pulmonary delivery in a mouse model of lung carcinoma. *J Control Release*. 2016;239:62–71. doi:10.1016/j.jconrel.2016.08.008
61. Suk JS, Xu Q, Kim N, Hanes J, Ensign LM. PEGylation as a strategy for improving nanoparticle-based drug and gene delivery. *Adv Drug Deliv Rev*. 2016;99:28–51. doi:10.1016/j.addr.2015.09.012
62. Abdelaziz HM, Gaber M, Abd-Elwakil MM, et al. Inhalable particulate drug delivery systems for lung cancer therapy: nanoparticles, microparticles, nanocomposites and nanoaggregates. *J Control Release*. 2018;269(November2017):374–392. doi:10.1016/j.jconrel.2017.11.036
63. Rytting E, Nguyen J, Wang X, Kissel T. Biodegradable polymeric nanocarriers for pulmonary drug delivery. *Expert Opin Drug Deliv*. 2008;5(6):629–639. doi:10.1517/17425247.5.6.629
64. Bertrand N, Wu J, Xu X, NazilaKamaly OF. Cancer nanotechnology: the impact of passive and active targeting in the era of modern cancer biology. *Adv Drug Deliv Rev*. 2014;66:2–25. doi:10.1016/J.ADDR.2013.11.009

65. Sanna V, Pala N, Sechi M. Targeted therapy using nanotechnology: focus on cancer. *Int J Nanomedicine*. 2014;9(1):467–483. doi:10.2147/IJN.S36654
66. Bar-Zeev M, Livney YD, Assaraf YG. Targeted nanomedicine for cancer therapeutics: towards precision medicine overcoming drug resistance. *Drug Resist Updat*. 2017;31:15–30. doi:10.1016/j.drup.2017.05.002
67. Dian L, Yu E, Chen X, et al. Enhancing oral bioavailability of quercetin using novel soluplus polymeric micelles. *Nanoscale Res Lett*. 2014;9(1):684. doi:10.1186/1556-276X-9-684

Supplementary material

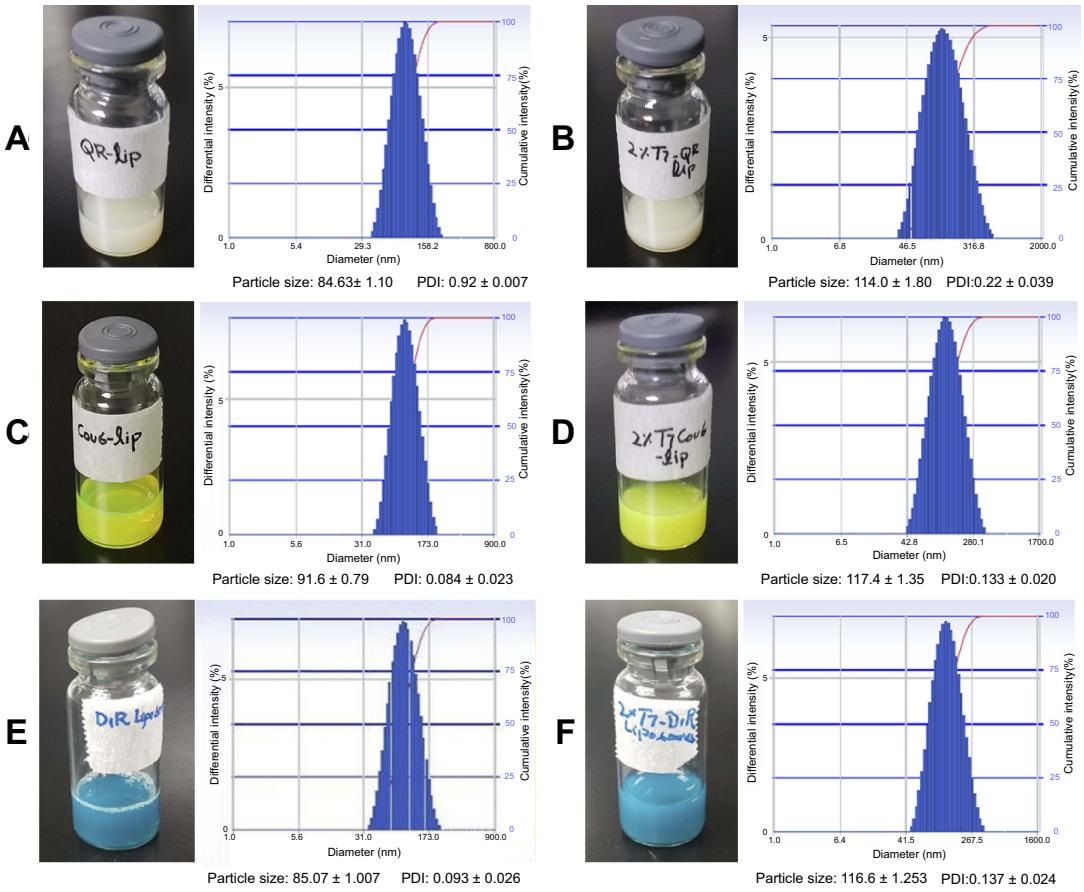

Figure S1 The appearance, particle-size distribution profile, particle size and polydispersity index (PDI) of various liposomes formulated. (**A**) QR-lip. (**B**) T7-QR-lip (2% T7 peptide density). (**C**) Cou6-lip. (**D**) T7-Cou6-lip (2% T7 peptide density). (**E**) DiR-lip. (**F**) T7-DiR-lip (2% T7 peptide density). Surface functionalization of liposomes (lip) containing quercetin (QR), Coumarin-6 (Cou6) and 1,1'-dioctadecyltetramethyl-indotricarbocyanine Iodide (DiR) with T7 peptide resulted in an increase in particle size and polydispersity index (PDI).

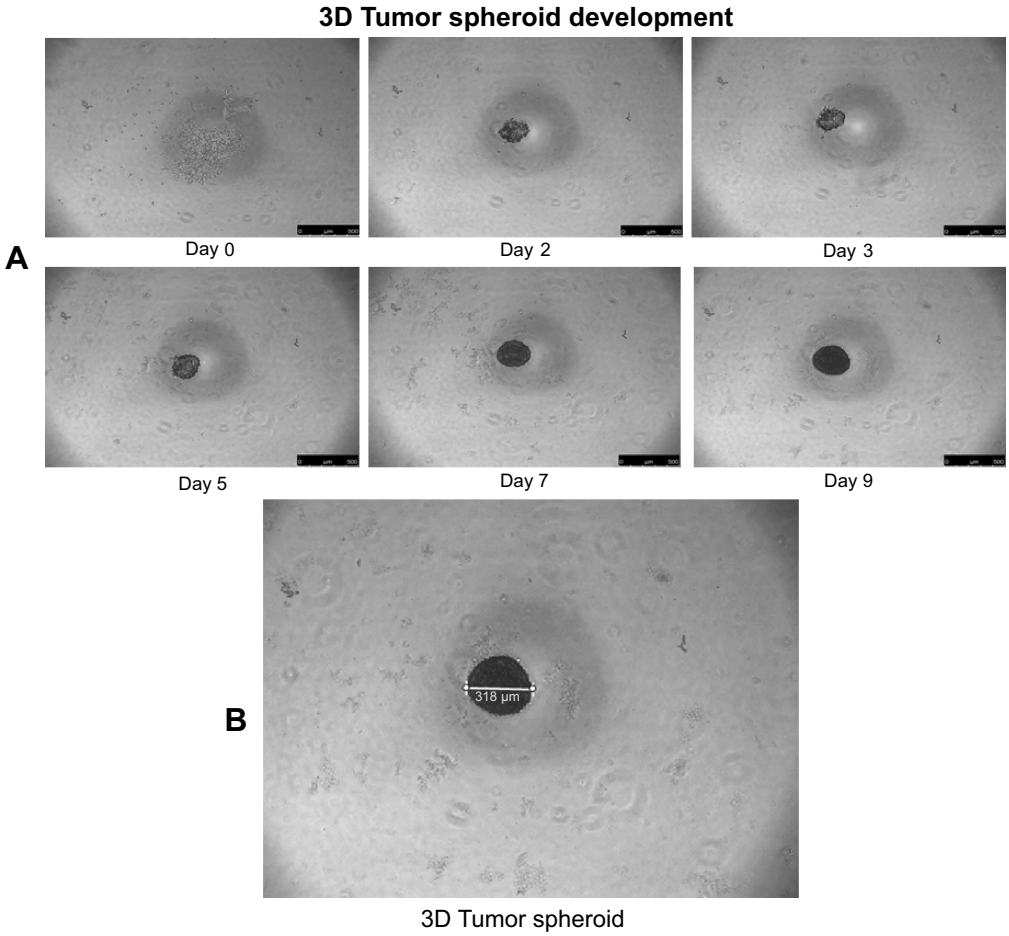

Figure S2 Representative bright-field images of A549 tumor-spheroid development. (**A**) Development of three-dimensional (3D) lung tumor spheroid at different time points (0, 2, 3, 5, 7 and 9 days). (**B**) Compact and uniform tumor spheroid (>300 µm) were selected for use in tumor-spheroid penetration and growth inhibition studies. The scale bar represents 500 µm. The bright-field images show that 3D lung tumor spheroids have been formed by the 2nd day, after incubation of A549 cells ($1x10^3$ cells in each well) in a 96-well plate precoated with 2% (w/v) agarose at 37 °C.

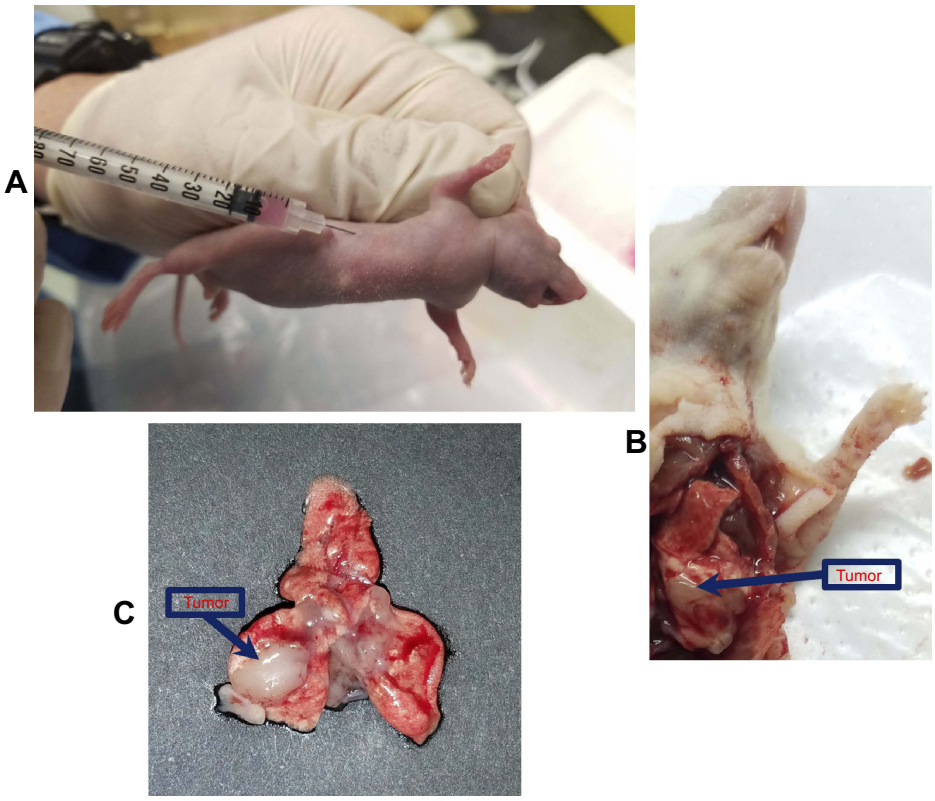

Figure S3 Establishment of the orthotopic lung tumor model in BALB/c nude mice. (**A**) Intrathoracic injection of A549-Luc cells to establish an orthotopic lung tumor model in mice. (**B**) Dissected mice showing solid tumor on the lungs after intrathoracic injection of A549-Luc cells. (**C**) Solid tumor on lungs surrounded by normal lung tissue, in the harvested lungs from orthotopic lung tumor-bearing mice. On the 7th day after A549-Luc cell intrathoracic injection, the lung tumor model was established in BALB/c nude mice.

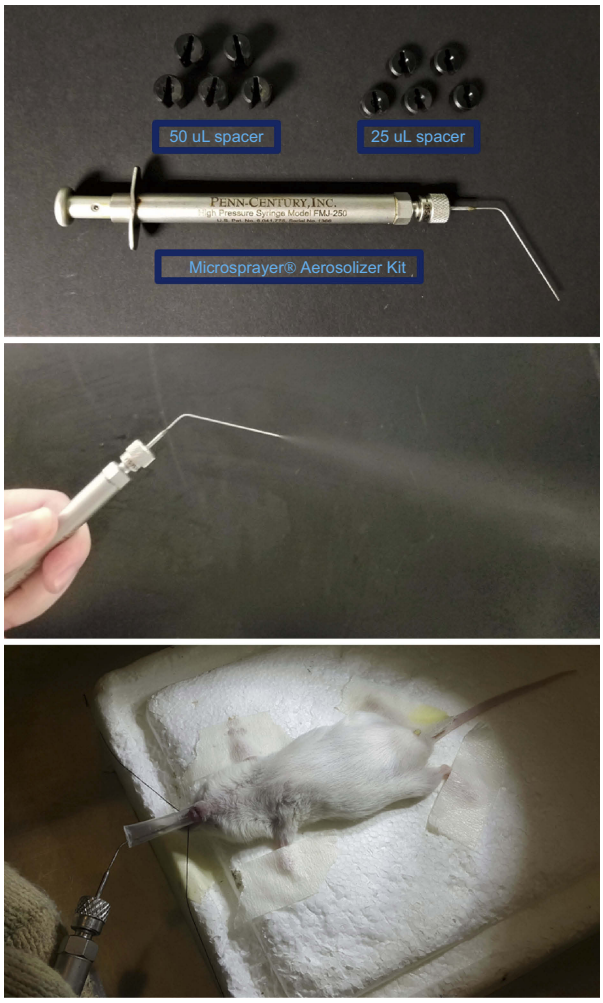

Figure S4 Endotracheal administration. (**A**) Microsprayer® Aerosolizer Pulmonary Aerosol-Kit for Mouse (Penn-Century Inc., PA, USA) with 25 µL and 50 µL spacers, for precise pulmonary administration of liquids (solution, suspension, etc.) (**B**) Microsprayer® Aerosolizer Pulmonary Aerosol-Kit in operation, generating the aerosol of a liquid for pulmonary administration. (**C**) Endotracheal administration of a liquid to the mouse using the Microsprayer® Aerosolizer Pulmonary Aerosol-Kit.